Table 2. Correlation between E_2 tissue concentrations and other variables in 20 human thymomas

	E_2 tissue concentration (pg/g)*	P †	r
EST immunoreactivity			
++ (n = 4)	27.0 ± 3.6	0.013	
+ (n = 8)	48.3 ± 7.5		
− (n = 8)	95.1 ± 15.8		
STS immunoreactivity			
++ (n = 3)	126.7 ± 32.9	0.008	
+ (n = 9)	65.7 ± 9.4		
− (n = 8)	35.5 ± 5.0		
17β-HSD type 1 immunoreactivity			
++ (n = 4)	125.5 ± 21.3	0.007	
+ (n = 7)	65.3 ± 7.7		
− (n = 9)	32.9 ± 3.3		
Aromatase mRNA level ‡			0.601 (P = 0.002)
ERα H-score ‡			0.774 (P < 0.001)
PR-B H-score ‡			0.749 (P = 0.001)
Clinical stage			
I (n = 9)	93.9 ± 14.3	0.006	
II (n = 5)	47.4 ± 5.7		
III (n = 3)	32.3 ± 4.9		
IV (n = 3)	25.3 ± 4.1		

*Mean ± SEM.
† P was listed only if significant. $P < 0.05$ was considered significant.
‡ Mean ± 95% confidence interval.

immunoreactivity of ERα and PR-B H-score and Ki-67 labeling index (LI) were done according to a previous report (3, 21, 22). Cases associated with a H-score of >50 were regarded as steroid receptor–positive thymomas (23).

Reverse transcription-PCR

RNA extraction and cDNA synthesis. Total RNA was extracted by homogenizing frozen tissue samples in 1 mL TRIzol reagent (Life Technologies, Inc., Grand Island, NY) followed by a phenol/chloroform phase extraction and isopropanol precipitation. The SuperScript Preamplification System RT kit (Life Technologies) was employed in the synthesis and amplification of cDNA according to the manufacturer's instructions.

Real-time reverse transcription-PCR. The Light Cycler System (Roche Diagnostics GmbH, Mannheim, Germany) was used to semiquantify the level of STS, EST, 17β-HSD type 1, and aromatase mRNA expression in 20 cases of thymoma using real-time PCR (24). Settings for the PCR thermal profile were as follows: initial denaturing step of 95°C for 1 minute followed by 40 cycles, respectively, of 95°C for 0 second, 15-second annealing at 58°C (EST) and 60°C (glyceraldehyde-3-phosphate dehydrogenase, STS, and aromatase), and extension for 15 seconds at 72°C. The primer sequences used in this study are as follows: EST (NM005420; forward 5-AGAGGAGCTTGTGGACAGGA-3 and reverse 5-GGCGACAATTTCTGGTTCAT-3; ref. 25), STS (M16505; forward 5-AGGGTCTGGGTGTGTCTGTC-3 and reverse 5-ACTGCAACGCCTACTTAAATG-3; ref. 26), 17β-HSD type 1 (XM 012644; forward 5′-AGGGCCGCGTGGACGTGCTGGTGTGTAAC-3′ and reverse 5′-CCATCAATCCTCCCACGCTCCCGG-3′; ref. 17), aromatase (X13589; forward 5′-GTGAAAAAGGGGACAAACAT-3′ and reverse 5′-TGGAATCGTCTCAGAAGTGT-3′; ref. 17), and glyceraldehyde-3-phosphate dehydrogenase (M33197; forward 5′-TGAACGGGAAGCTCACTGG-3′ and reverse 5′-TCCACCACCCTGTTGCTGTA-3′; ref. 3). Liver (25) cells were used as a positive control for EST, whereas frozen tissues of placenta were used as a positive control for STS (26, 27), 17β-HSD type 1, and aromatase (17). Negative control experiments lacked cDNA substrate to check for the presence of exogenous contaminant DNA. No amplified products were observed under these conditions and PCR products were purified and subjected to direct sequencing to verify amplification of the correct sequences as described previously. The mRNA levels for STS, EST, and aromatase in each case are summarized as a ratio of glyceraldehyde-3-phosphate dehydrogenase and evaluated as a ratio (%) compared with that of each positive control.

Statistical analysis. Values for patient age, tumor size, Ki-67 LI, H-scores of ERα or PR-B, and mRNA levels for EST, STS, 17β-HSD type 1, or aromatase were summarized as a mean ± 95% confidence interval. Statistical analyses between E_2 tissue concentration and aromatase mRNA level, ERα H-score, or PR-B H-score were done using a correlation coefficient (r) and regression equation. An association between immunoreactivity for EST, STS, or 17β-HSD type 1 and these variables were evaluated using Kruskal-Wallis tests. Statistical differences between immunoreactivity of EST, STS, or 17β-HSD type 1 and sex, status of myasthenia gravis, clinical stage, or WHO histologic classification were evaluated in a cross-table using the χ^2 test. Overall survival curves were generated according to the Kaplan-Meier method, and the statistical significance was calculated using the log-rank test. Univariate and multivariate analyses were evaluated by a proportional hazard model (Cox) using PROC PHREG in SAS software. $P < 0.05$ was considered significant.

Results

Cell proliferation assay. E_2 inhibits cell proliferation of TEC in proportion to the concentration of E_2 (10, 100, and 1,000 nmol/L; $P < 0.001$; Fig. 1A). ICI 182,780, which is a steroidal anti-estrogen with no agonist activities, blocks inhibition of cell proliferation exerted by E_2 (Fig. 1B; ref. 28). Terminal deoxynucleotidyl transferase–mediated dUTP nick end labeling

analysis showed few apoptotic cells after treatment of E_2 (data not shown).

Estrone and estradiol synthesis in primary culture of thymoma-derived neoplastic epithelial cells. E_1 and E_2 production in primary cultures of TEC are summarized in Fig. 2. E_1 and E_2 concentrations are detected in proportion to the duration and concentration of E_1-S. Concentrations of E_1 and E_2 in the medium of TEC treated with E_1-S (2.5 and 12.5 nmol/L) were significantly higher than those with E_1-S of 0.5 nmol/L after 8 and 24 hours ($P < 0.05$). E_1 and E_2 concentrations in phenol red and FBS-free DMEM were below the limits of detection.

Correlation among estradiol concentrations and estrogen sulfotransferase, steroid sulfatase, or 17β-hydroxysteroid dehydrogenase type 1 immunoreactivity, aromatase mRNA level, estrogen receptor α and progesterone receptor-B H-score, and clinical stage in 20 human thymomas. Results are summarized in Table 2. E_2 concentrations in thymoma were significantly higher than those of normal thymus (59.3 ± 9.5 versus 19.2 ± 3.6; $P < 0.05$), inversely correlated with that of EST

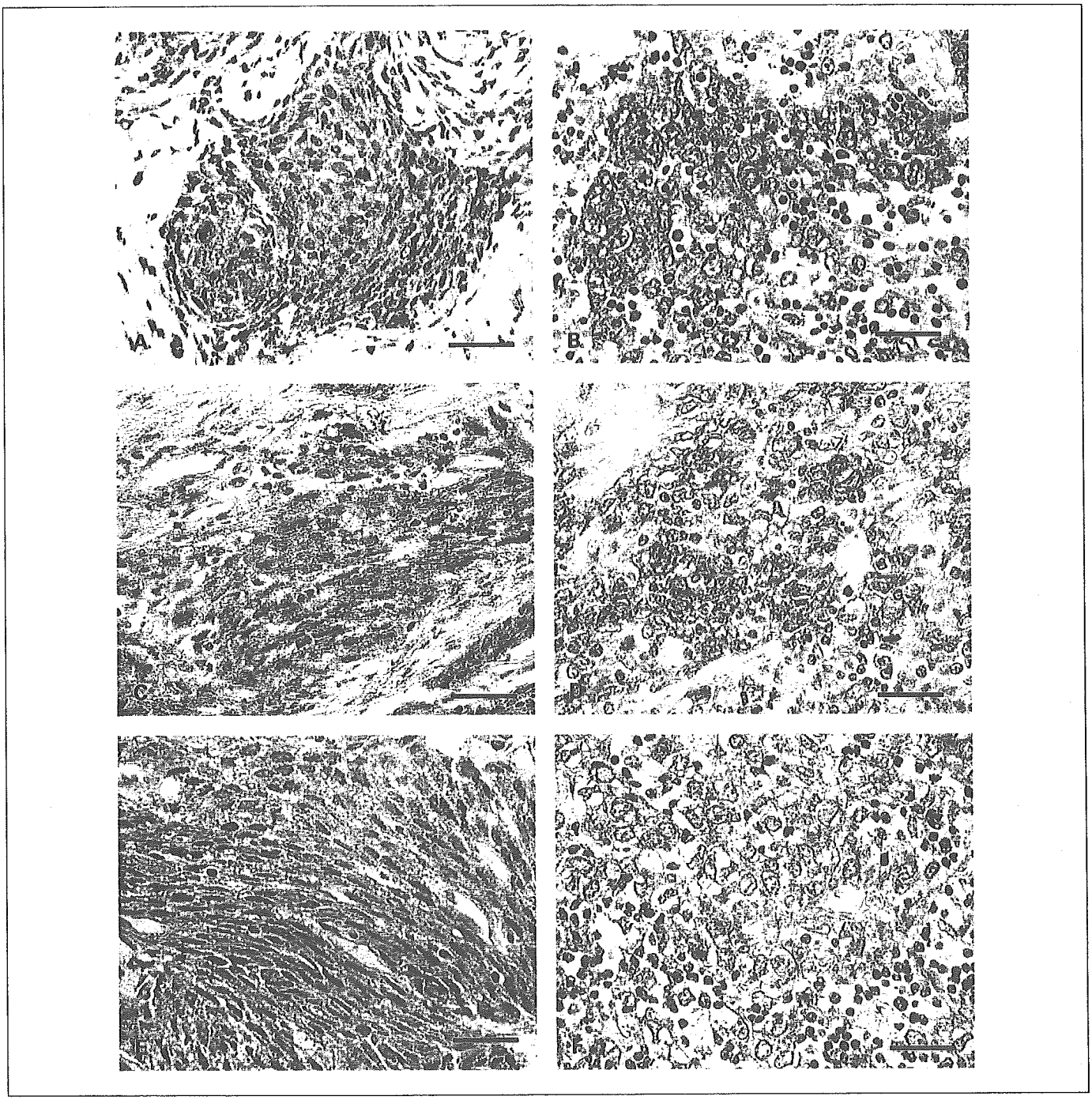

Fig. 3. Immunohistochemistry for EST (*A* and *B*), STS (*C* and *D*), and 17β-HSD type 1 (*E* and *F*) in tissue specimens of human thymoma. Immunoreactivity for EST, STS, and 17β-HSD type 1 was detected in the cytoplasm of TEC but not in lymphocytes. *A*, *C*, and *E*, type A by WHO classification (same field); *B*, *D*, and *F*, type B3 (same field). Original magnification, ×400. Bar, 25 μm.

Table 3. Correlation between EST, STS, and 17β-HSD type 1 immunoreactivity and pathologic variables in 132 human thymomas

	EST immunoreactivity			P	STS immunoreactivity		
	++ (*n* = 22)	+ (*n* = 55)	− (*n* = 55)		++ (*n* = 20)	+ (*n* = 57)	− (*n* = 55)
Age (y)*	50.0 ± 3.7	57.2 ± 1.8	51.4 ± 2.0	0.290	53.6 ± 3.6	54.0 ± 1.9	51.6 ± 2.1
Sex							
Male	7 (31.8)	32 (58.2)	19 (34.5)	0.405	12 (60.0)	24 (42.1)	22 (40.0)
Female	15 (68.2)	23 (41.8)	36 (65.5)		8 (40.0)	33 (57.9)	33 (60.0)
Pre	5 (22.7)	11 (20.0)	22 (40.0)	0.138	5 (25.0)	16 (28.1)	17 (30.9)
Post	10 (45.5)	12 (21.8)	14 (25.5)		3 (15.0)	17 (29.8)	16 (29.1)
Myasthenia gravis							
+	2 (9.1)	13 (23.6)	10 (18.2)	0.333	8 (40.0)	9 (15.8)	8 (14.5)
−	20 (90.9)	42 (76.4)	45 (81.8)		12 (60.0)	48 (84.2)	47 (85.5)
Tumor size (mm)*	78.0 ± 6.5	58.7 ± 3.3	54.8 ± 3.0	0.013	50.6 ± 3.5	62.2 ± 3.6	61.8 ± 3.6
Clinical stage							
I	2 (9.1)	17 (30.9)	44 (80.0)	<0.001	12 (60.0)	33 (57.9)	18 (32.7)
II	2 (9.1)	21 (38.2)	9 (16.4)		5 (25.0)	14 (24.6)	13 (23.6)
III	4 (18.2)	16 (29.1)	1 (1.8)		2 (10.0)	4 (7.0)	15 (27.3)
IV	14 (63.6)	1 (1.8)	1 (1.8)		1 (5.0)	6 (10.5)	9 (16.4)
Ki-67 LI*	3.2 ± 0.2	1.6 ± 0.1	1.3 ± 0.1	0.045	1.42 ± 0.13	1.58 ± 0.11	2.11 ± 0.13
Aromatase mRNA level (%), *n* = 20	5.12 ± 0.21	3.56 ± 0.11	1.24 ± 0.24	0.029	1.99 ± 0.51	3.32 ± 1.42	2.43 ± 0.96
ERα *H*-score*	46.3 ± 10.4	71.5 ± 7.9	93.3 ± 4.2	0.009	105.3 ± 1.8	83.6 ± 4.9	54.4 ± 7.7
PR-B *H*-score*	22.3 ± 11.0	46.3 ± 9.6	68.4 ± 6.2	0.015	83.0 ± 1.2	56.4 ± 7.6	31.1 ± 8.4

NOTE: $P < 0.05$ was considered significant.
Abbreviations: Pre, premenopausal; Post, postmenopausal.
*Mean ± 95% confidence interval. All other values represent mean ± SE.

immunoreactivity ($P = 0.013$), and positively correlated with that of STS ($P = 0.008$), 17β-HSD type 1 ($P = 0.007$), aromatase mRNA level ($r = 0.601$; $P = 0.002$), ERα *H*-score ($r = 0.774$; $P < 0.001$), and PR-B *H*-score ($r = 0.749$; $P = 0.001$). E_2 concentrations were significantly higher in cases with earlier clinical stage ($P = 0.006$).

Immunolocalization of estrogen sulfotransferase, steroid sulfatase, and 17β-hydroxysteroid dehydrogenase type 1 in human thymoma. EST immunoreactivity was detected predominantly in the cytoplasm of epithelial cells of thymoma (Fig. 3A) but not in lymphocytes (Fig. 3B). The number of the cases positive for EST in 132 human thymomas was summarized as follows: ++, $n = 22$ (16.6%); +, $n = 55$ (41.7%); and −, $n = 55$ (41.7%).

STS immunoreactivity was also detected predominantly in the cytoplasm of epithelial cells of thymoma (Fig. 3C) but not in lymphocytes (Fig. 3D). The number of cases positive for STS immunoreactivity was summarized as follows: ++, $n = 20$ (15.2%); +, $n = 57$ (43.2%); and −, $n = 55$ (41.6%).

17β-HSD type 1 immunoreactivity was detected predominantly in the cytoplasm of epithelial cells of thymoma (Fig. 3E) but not in lymphocytes (Fig. 3F). The number of cases positive for 17β-HSD type 1 immunoreactivity in these cases was summarized as follows: ++, $n = 27$ (20.5%); +, $n = 46$ (34.8%); and −, $n = 59$ (44.7%).

Real-time PCR analysis. mRNA expression of EST, STS, 17β-HSD type 1, aromatase, and glyceraldehyde-3-phosphate dehydrogenase was identified as a specific single band at 114, 290, 201, 215, and 307 bp, respectively (data not shown). There were significant positive correlations between EST immunoreactivity and its mRNA level ($P = 0.001$), STS immunoreactivity and its mRNA level ($P = 0.010$), and 17β-HSD type 1 immunoreactivity and its mRNA level ($P = 0.007$; data not shown).

Correlation between estrogen sulfotransferase, steroid sulfatase, and 17 β-hydroxysteroid dehydrogenase type 1 immunoreactivity and clinicopathologic variables. An association between EST, STS, or 17β-HSD type 1 immunoreactivity and clinicopathologic factors in thymoma patients were summarized in Table 3. EST immunoreactivity was positively correlated with tumor size ($P = 0.013$), clinical stage of the patients ($P < 0.001$), Ki-67 LI ($P = 0.045$), and mRNA level of aromatase ($P = 0.029$). EST immunoreactivity was inversely correlated with ERα *H*-score ($P = 0.009$) and PR-B *H*-score ($P = 0.015$).

There were significant inverse correlations between STS immunoreactivity and clinical stage of the patients ($P = 0.036$) or Ki-67 LI ($P = 0.011$). There were significant positive correlations between STS immunoreactivity and ERα *H*-score ($P = 0.005$) or PR-B *H*-score ($P = 0.006$).

There were significant inverse correlations between 17β-HSD type 1 immunoreactivity and clinical stage of the patients

Table 3. Correlation between EST, STS, and 17β-HSD type 1 immunoreactivity and pathologic variables in 132 human thymomas (Cont'd)

P	17β-HSD type 1 immunoreactivity			P
	++ (n = 27)	+ (n = 46)	− (n = 59)	
0.697	56.8 ± 2.8	53.7 ± 2.0	50.6 ± 2.1	0.191
0.286	10 (37.0)	21 (45.7)	27 (45.8)	0.720
	17 (63.0)	25 (54.3)	32 (54.2)	
0.572	7 (25.9)	13 (28.3)	18 (30.5)	0.138
	10 (37.1)	12 (26.0)	14 (23.7)	
0.053	9 (33.3)	11 (23.9)	15 (25.4)	0.141
	18 (67.7)	35 (76.1)	44 (74.6)	
0.185	56.9 ± 4.6	53.3 ± 3.0	60.3 ± 3.7	0.076
0.036	14 (51.9)	28 (60.9)	21 (35.6)	0.008
	9 (33.3)	12 (26.1)	11 (18.6)	
	2 (7.4)	3 (6.5)	16 (27.1)	
	2 (7.4)	3 (6.5)	11 (18.6)	
0.011	1.50 ± 0.13	1.47 ± 0.11	2.07 ± 0.14	0.012
0.539	3.11 ± 0.82	2.58 ± 1.21	1.88 ± 1.02	0.053
0.005	103.3 ± 2.2	86.4 ± 3.6	53.9 ± 6.6	0.001
0.006	78.5 ± 3.8	64.9 ± 6.4	26.4 ± 6.4	0.001

(P = 0.008) or Ki-67 LI (P = 0.005) and positive correlations between 17β-HSD type 1 immunoreactivity and ERα H-score (P = 0.001) or PR-B H-score (P = 0.001).

Correlation between WHO classification and other variables. An association between WHO classification and clinicopathologic factors in thymoma patients was summarized in Table 4. E_2 concentrations were significantly higher in type A thymoma than type B thymoma (P = 0.005). There was a significant positive correlation between WHO classification and EST immunoreactivity (P < 0.001) and inverse correlations between WHO classification and STS immunoreactivity (P < 0.001), ERα H-score (P = 0.015), or PR-B H-score (P = 0.028).

Correlation between estrogen sulfotransferase, steroid sulfatase, and 17β-hydroxysteroid dehydrogenase type 1 immunoreactivity and overall survival of patients with thymoma. There was a significant positive correlation between EST immunoreactivity and clinical outcome of the patients (P = 0.0001; Fig. 4A). No significant correlations were detected between STS or 17β-HSD type 1 immunoreactivity and clinical outcome in patients with thymoma (Fig. 4B and C).

Following a univariate analysis (Table 5), clinical stage (P = 0.0017), ERα immunoreactivity (P = 0.0021), EST immunoreactivity (P = 0.0023), and tumor size (P = 0.0024) all turned out to be significant prognostic factors of overall survival in 132 thymoma patients. A subsequent multivariate analysis revealed that only clinical stage (P = 0.0239), ERα immunoreactivity (P = 0.0355), and EST immunoreactivity (P = 0.0436) were independent prognostic factors with relative risks of >1.0 in our series of 132 thymoma patients.

Discussion

Estrogens have been considered to play important roles in biological features of thymoma. However, this is the first study to show an inhibition of thymic epithelial cell proliferation by estrogens, the presence of *in situ* production of estrogens in human thymoma using primary cell culture, and a correlation between the status of estrogen metabolizing or producing enzymes and clinicopathologic variables or endogenous estrogen concentrations in human thymus and thymoma.

In our present study, TEC proliferation was inhibited by E_2 via ERα. This finding is consistent with our previous study, which suggests that E_2 or E_2-like agents may be effective in treatment of thymoma, especially in cases of inoperable or disseminated tumor possibly through suppressing its cell proliferation activity (3). In this study, E_1 and E_2 were both produced from E_1-S in ERα, STS, and 17β-HSD type 1 positive TEC in proportion to the duration and concentration of E_1-S administered. In addition, E_2 tissue concentrations were inversely correlated with the status of EST immunoreactivity, positively correlated with the status of STS or 17β-HSD type 1 immunoreactivity, and significantly higher in earlier clinical stages and lower histologic grades. These findings showed that lower histologic grade tumors or well-differentiated thymoma cells were associated with *in situ* estrogen biosynthesis and estrogenic actions via binding to ERα, which result in E_2-dependent inhibition of tumor growth.

EST immunoreactivity was also detected in TEC and positively correlated with Ki-67 LI or tumor size and inversely correlated

Table 4. Correlation between WHO classification and other variables in human thymomas

	A	AB	B1	B2	B3	P*
E_2 tissue concentration (pg/g) †	111.5 ± 27.8	89.5 ± 9.0	31.5 ± 5.2	34.0 ± 5.2	28.7 ± 2.6	0.005
EST immunoreactivity						
++ (*n* = 22)	2 (9.1)	1 (4.5)	1 (4.5)	7 (31.8)	11 (50.0)	<0.001
+ (*n* = 55)	14 (25.5)	12 (21.8)	8 (14.5)	17 (30.9)	4 (7.3)	
− (*n* = 55)	10 (18.7)	12 (21.8)	20 (36.4)	12 (21.8)	1 (1.8)	
STS immunoreactivity						
++ (*n* = 22)	11 (55.0)	3 (15.0)	2 (10.0)	3 (15.0)	1 (5.0)	<0.001
+ (*n* = 55)	14 (24.6)	14 (24.6)	15 (26.3)	10 (17.5)	4 (7.0)	
− (*n* = 55)	1 (1.8)	8 (14.5)	12 (21.8)	23 (41.8)	11 (20.0)	
17β-HSD type 1 immunoreactivity						
++ (*n* = 27)	11 (40.8)	3 (11.1)	4 (14.8)	6 (22.2)	3 (11.1)	0.057
+ (*n* = 46)	8 (17.4)	11 (23.9)	11 (23.9)	14 (30.4)	2 (4.4)	
− (*n* = 59)	7 (11.9)	11 (18.6)	14 (23.7)	16 (27.2)	11 (18.6)	
Aromatase mRNA level †	3.11 ± 0.12	3.42 ± 0.22	3.24 ± 0.18	2.98 ± 0.32	3.98 ± 0.22	0.283
ERα *H*-score †	111.1 ± 9.8	104.9 ± 16.2	96.3 ± 14.4	64.9 ± 12.6	36.5 ± 7.4	0.015
PR-B *H*-score †	85.7 ± 15.8	64.6 ± 14.0	51.3 ± 11.9	45.1 ± 9.8	18.0 ± 9.6	0.028

*P was listed only if significant. $P < 0.05$ was considered significant.
† Mean ± 95% confidence interval. All other values represent mean ± SE.

with *H*-score of ERα or PR-B. In addition, EST-positive thymoma patients tended to be associated with advanced clinical stages with higher histologic grades and significantly adverse clinical outcome than EST-negative thymoma. In addition, EST immunoreactivity was shown to be an independent prognostic factor for overall survival as well as ERα and clinical stage following multivariate analysis. Tissue E_2 concentrations were also inversely correlated with EST immunoreactivity. Therefore, EST-negative thymoma is considered to result in an increased *in situ* concentration of biologically active estrogens, which may

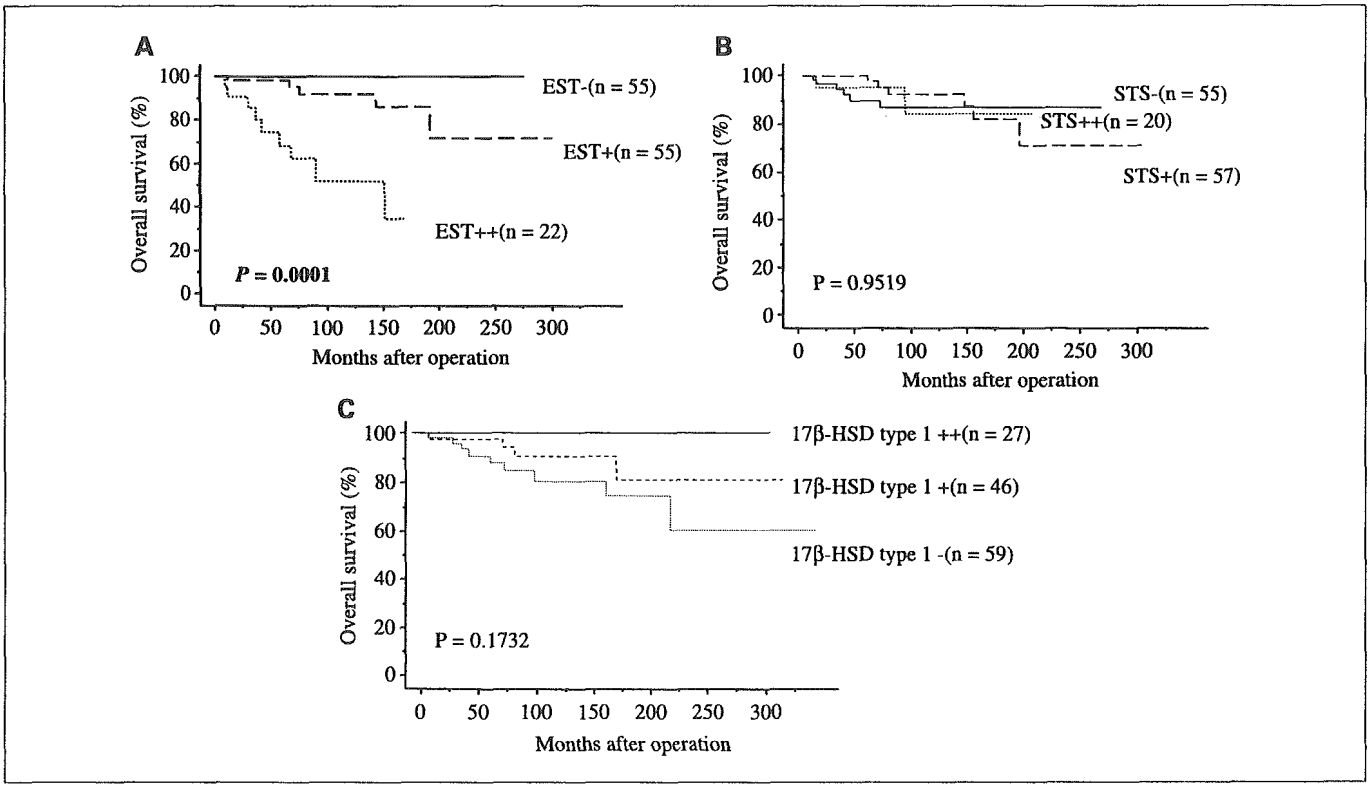

Fig. 4. Overall survival of 132 patients with thymoma with respect to EST (*A*), STS (*B*), and 17β-HSD type 1 (*C*) immunoreactivity (Kaplan-Meier method). EST immunoreactivity was significantly associated with an improved overall survival ($P = 0.0001$) but STS and 17β-HSD type 1 immunopositive thymoma was relatively associated with better clinical outcome, although this association did not reach statistical significance.

Table 5. Univariate and multivariate analyses of overall survival in 132 thymoma patients

Variable	Univariate	Multivariate	
	P	*P*	Relative risk (95% confidence interval)
Clinical stage (II, III, IV/I)	0.0017	0.0239	5.783 (1.709-47.196)
ERα (−/+)	0.0021	0.0355	4.786 (1.143-21.959)
EST (++, +/−)	0.0023	0.0436	2.509 (1.126-5.263)
Tumor size (>60/≦60 mm)	0.0024		
Female (premenopausal/postmenopausal)	0.0620		
PR-B (−/+)	0.4694		
Sex (male/female)	0.7033		

contribute to inhibition of cell proliferation in thymoma through ERα. Qian et al. showed that MCF-7 breast cancer cells transfected with EST expressed EST at levels similar to those observed in normal human mammary epithelial cells and are associated with much lower estrogen-stimulated DNA synthesis or cell proliferation than MCF-7 cells not associated with EST expression (29). EST-negative breast cancer is therefore considered to be associated with an increased *in situ* estrogen concentration, which results in an increased incidence of tumor recurrence and subsequent poor clinical outcome for the patients diagnosed with breast cancer (20, 30). EST is more frequently detected in TEC in higher histologic grades or advanced clinical stages, which are consistent with decreased expression of STS or 17β-HSD type 1. All of these are considered to result in decreased levels of E_2 in these thymoma cases. STS and 17β-HSD type 1 immunoreactivity was also positively correlated with the *H*-score of ERα and PR-B and inversely correlated with Ki-67 LI. STS-positive and 17β-HSD type 1−positive thymoma cases were significantly correlated with earlier clinical stages and lower histologic grades. In addition, 17β-HSD type 1−positive thymoma tends to be associated with favorable clinical outcome. STS catalyzes E_1-S to E_1 and 17β-HSD type 1 catalyzes E_1 to E_2 in human thymoma, which contributes to increase *in situ* estrogen concentration (31, 32). Results of our present study suggest that STS and 17β-HSD type 1 also contribute to estrogenic actions in human thymoma through *in situ* estrogen production. In contrast, a significant inverse correlation was reported between 17β-HSD type 1 immunoreactivity and Ki-67 LI or histologic grade in patients with breast cancer (33, 34). 17β-HSD type 1 immunoreactivity is considered to reflect its enzymatic activity (16), and ER immunoreactivity has been shown to be correlated with estrogen-dependent biological phenomena (35). Therefore, results of our present study showed that *in situ* produced E_2 exerts its effects through ERα in human thymoma, which may be consistent with the relatively better clinical outcome of 17β-HSD type 1−positive human thymoma patients. Further investigations are required for clarification.

PR-B *H*-score was positively correlated with STS and 17β-HSD type 1 immunoreactivity and inversely correlated with EST immunoreactivity in human thymoma. These findings are also consistent with the fact that expression of PR is estrogen related, because PR has been regarded as one of the markers of a functional estrogen pathway (36) and ERα-positive thymomas are generally positive for PR-B (3). The levels of immunoreactive EST and EST mRNA in Ishikawa cells, a cell line established from human endometrial adenocarcinoma, were both shown to be increased by progesterone. These results suggest that progesterone is capable of specifically inducing EST and estrogen sulfation in the human Ishikawa endometrial adenocarcinoma cell line (37). Furthermore, progestin has also been reported to induce 17β-HSD enzyme protein in the T-47D

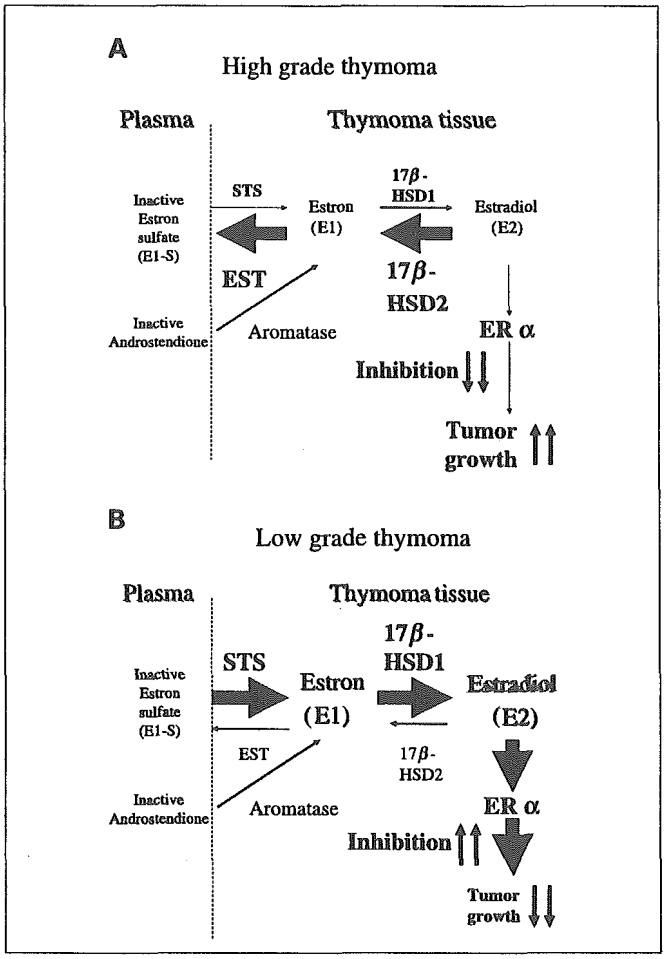

Fig. 5. Summary of local production of estrogens in high-grade (*A*) and low-grade (*B*) thymoma. High concentrations of circulating inactive steroids, androstenedione and E_1-S, are major precursor substrates of local estrogen production in these tissues. Aromatase catalyzes androstenedione into E_1, and STS hydrolyzes E_1-S to E_1. E_1 is subsequently converted to potent E_2 by 17β-HSD type 1 and acts on TEC via ERα. EST sulfonates E_1 to biologically inactive E_1-S. High intratumoral E_2 concentration as a result of *in situ* production in thymoma with early-stage or well-differentiated histologic features is therefore considered to result in inhibition of cell proliferation of TEC.

human breast cancer cell line (38). Therefore, coexpression of EST, STS, and/or 17β-HSD type 1 and PR detected thymoma in this study suggests that progesterone may play an important role in regulating the expression of these enzymes involved in *in situ* estrogen metabolism in thymoma. However, it awaits further investigating to identify the specific roles of these enzymes in metabolizing estrogens in thymoma.

Aromatase cytochrome *P450* (*CYP19* gene) is an enzyme located in the endoplasmic reticulum of estrogen-producing cells and a key enzyme mainly involved in the aromatization of androstenedione to E_1 (29). In the present study, there was a statistically significant positive correlation between aromatase mRNA level and immunoreactivity for EST but not for STS, 17β-HSD type 1, and aromatase mRNA levels tended to correlate with E_2 tissue concentrations. These results also suggest that estrogen can still be produced via aromatase pathway in EST-positive thymoma case even if the activity of aromatase was 0.5% to 2% of STS (3).

We show the findings of *in situ* estrogen production in human thymoma (Fig. 5). Advanced stage or high-grade thymoma produces low level of E_2, which cannot inhibit the proliferation of TEC (Fig. 5A). On the other hand, high concentration of E_2 is produced in early-stage or low histologic grade thymoma and inhibits the proliferation of TEC (Fig. 5B).

In summary, high intratumoral E_2 concentration as a result of *in situ* production in thymoma with early-stage or well-differentiated histologic features is therefore considered to result in inhibition of cell proliferation of TEC.

Acknowledgments

We thank Drs. Touichirou Takizawa and Takumi Akashi (Department of Pathology, Graduate School, Tokyo Medical and Dental University) and Dr. Hideki Akamatsu (Department of Thoracic Cardiovascular Surgery, Graduate School, Tokyo Medical and Dental University) for their kind efforts in retrieving the specimens of thymoma and Andrew D. Darnel (Department of Pathology, Tohoku University School of Medicine) for careful editing of this article.

References

1. Alexieva-Figusch J, Van Putten WL, Blankenstein MA, Blonk-Van Der Wijst J, Klijn JG. The prognostic value and relationships of patient characteristics, estrogen and progesterone receptors, and site of relapse in primary breast cancer. Cancer 1988;61:758–68.
2. Pasqualini JR, Chetrite G, Blacker C. Concentrations of estrone, estradiol, and estrone sulfate and evaluation of sulfatase and aromatase activities in pre- and postmenopausal breast cancer patients. J Clin Endocrinol Metab 1996;81:1460–4.
3. Ishibashi H, Suzuki T, Suzuki S, et al. Sex steroid hormone receptors in human thymoma. J Clin Endocrinol Metab 2003;88:2309–17.
4. Ruder HJ, Loriau L, Lipsett MB. Estrone sulfate: production rate and metabolism in man. J Clin Invest 1972;51:1020–33.
5. Samojlik E, Santen RJ, Worgul TJ. Plasma estrone sulfate: assessment of reduced estrogen production during treatment of metastatic breast carcinoma. Steroids 1982;39:497–507.
6. Naitoh K, Honjo H, Yamamoto T, et al. Estrone sulfatase and sulfotransferase activity in human breast cancer and endometrial cancer. J Steroid Biochem 1989;33:1049–54.
7. Pasqualini JR, Gelly C. Biological response of the antiestrogen ICI 164,384 in human hormone-dependent and hormone-independent mammary cancer cell lines. Cancer Lett 1990;50:133–9.
8. Miller WR, Hawkins RA, Forrest AM. Significance of aromatase activity in human breast cancer. Cancer Res 1982;42:3365–8.
9. Luu-The V, Labrie C, Zhao HF, et al. Characterization of cDNAs for human estradiol 17β-dehydrogenase and assignment of the gene to chromosome 17: evidence for two mRNA species with distinct 59-termini in human placenta. Mol Endocrinol 1989;3:1301–9.
10. Falany CN. Enzymology of human cytosolic sulfotransferase. FASEB J 1997;11:206–16.
11. Kadota Y, Okumura M, Miyoshi S, et al. Altered T-cell development in human thymoma is related to impairment of MHC class II transactivator expression induced by interferon-γ (IFN-γ). Clin Exp Immunol 2000;121:59–68.
12. Salakou S, Tsamandas AC, Bonikos DS, et al. The potential role of bcl-2, bax, and Ki67 expression in thymus of patients with myasthenia gravis, and their correlation with clinicopathologic parameters. Eur J Cardiothorac Surg 2001;20:712–21.
13. Yamakawa Y, Masaoka A, Hashimoto T, et al. A tentative tumor-node-metastasis classification of thymoma. Cancer 1991;68:1984–7.
14. Rosai J, Sobin LH. Histological typing of tumours of the thymus. International histological classification of tumours. 2nd ed. New York: Springer; 1999. p. 9–13.
15. Saeki T, Takashima S, Sasaki H, Salomon DS. Localization of estrone sulfatase in human breast carcinoma. Breast Cancer 1999;6:331–7.
16. Poutanen M, Isomaa V, Lehto VP, Vihko R. Immunological analysis of 17β-hydroxysteroid dehydrogenase in benign and malignant human breast tissue. Int J Cancer 1992;50:386–90.
17. Sasano H, Frost AR, Saitoh R, et al. Aromatase and 17β-hydroxysteroid dehydrogenase type 1 in human breast carcinoma. J Clin Endocrinol Metab 1996;81:4042–6.
18. Miki Y, Nakata T, Suzuki T, et al. Systemic distribution of steroid sulfatase and estrogen sulfotransferase in human adult and fetal tissues. J Clin Endocrinol Metab 2002;87:5760–8.
19. Takeyama J, Sasano H, Suzuki T, Iinuma K, Nagura H, Andersson S. 17β-Hydroxysteroid dehydrogenase types 1 and 2 in human placenta: an immunohistochemical study with correlation to placental development. J Clin Endocrinol Metab 1998;83:3710–5.
20. Suzuki T, Nakata T, Miki Y, et al. Estrogen sulfotransferase and steroid sulfatase in human breast carcinoma. Cancer Res 2003;63:2762–70.
21. Goulding H, Pinder S, Cannon P, et al. A new immunohistochemical antibody for the assessment of estrogen receptor status on routine formalin-fixed tissue samples. Hum Pathol 1995;26:291–4.
22. Pan CC, Ho DM, Chen WY, Huang CW, Chiang H. Ki-67 labeling index correlates with stage and histology but not significantly with prognosis in thymoma. Histopathology 1998;33:453–8.
23. Thike AA, Chng MJ, Fook-Chong S, Tan PH. Immunohistochemical expression of hormone receptors in invasive breast carcinoma: correlation of results of *H*-score with pathological parameters. Pathology 2001;33:21–5.
24. Dumoulin FL, Nischalke HD, Leifeld L, et al. Semiquantification of human C-C chemokine mRNAs with reverse transcription/real-time PCR using multi-specific standards. J Immunol Methods 2000;241:109–19.
25. Aksoy IA, Wood TC, Weinshilboum R. Human liver estrogen sulfotransferase: identification by cDNA cloning and expression. Biochem Biophys Res Commun 1994;200:1621–9.
26. Utsumi T, Yoshimura N, Takeuchi S, et al. Steroid sulfatase expression is an independent predictor of recurrence in human breast cancer. Cancer Res 1999;59:377–81.
27. Salido EC, Yen PH, Barajas L, Shapiro LJ. Steroid sulfatase expression in human placenta: immunocytochemistry and *in situ* hybridization study. J Clin Endocrinol Metab 1990;70:1564–7.
28. Wakeling AE, Dukes M, Bowler J. A potent specific pure antiestrogen with clinical potential. Cancer Res 1991;51:3867–73.
29. Qian Y, Deng C, Song WC. Expression of estrogen sulfotransferase in MCF-7 cells by cDNA transfection suppresses the estrogen response: potential role of the enzyme in regulating estrogen-dependent growth of breast epithelial cells. J Pharmacol Exp Ther 1998;286:555–60.
30. Suzuki T, Moriya T, Ishida T, Kimura M, Ohuchi N, Sasano H. *In situ* production of estrogens in human breast carcinoma. Breast Cancer 2002;9:296–302.
31. Selcer KW, Hegde PV, Li PK. Inhibition of estrone sulfatase and proliferation of human breast cancer cells by nonsteroidal (*p*-*O*-sulfamoyl)-*N*-alkanoyl tyramines. Cancer Res 1997;57:702–7.
32. Pasqualini JR, Chetrite GS. Estrone sulfatase versus estrone sulfotransferase in human breast cancer: potential clinical applications. J Steroid Biochem Mol Biol 1999;69:287–92.
33. Suzuki T, Moriya T, Ariga N, Kaneko C, Kanazawa M, Sasano H. 17β-hydroxysteroid dehydrogenase type 1 and type 2 in human breast carcinoma: a correlation to clinicopathological parameters. Br J Cancer 2000;82:518–23.
34. Sasano H, Suzuki T, Takeyama J, et al. 17-β-Hydroxysteroid dehydrogenase in human breast and endometrial carcinoma. A new development in intracrinology. Oncology 2000;59 Suppl 1:5–12.
35. Marrazzo A, La Bara G, Taormina P, Bazan P. Determination of oestrogen receptors with monoclonal antibodies in fine needle aspirates of breast carcinoma. Br J Cancer 1989;59:426–8.
36. Horwitz KB, McGuire WL. Estrogen control of progesterone receptor in human breast cancer. Correlation with nuclear processing of estrogen receptor. J Biol Chem 1978;253:2223–8.
37. Falany JL, Falany CN. Regulation of estrogen sulfotransferase in human endometrial adenocarcinoma cells by progesterone. Endocrinology 1996;137:1395–401.
38. Poutanen M, Isomaa V, Kainulainen K, Vihko R. Progestin induction of 17 β-hydroxysteroid dehydrogenase enzyme protein in the T-47D human breast-cancer cell line. Int J Cancer 1990;46:897–901.

Splicing potentiation by growth factor signals via estrogen receptor phosphorylation

Yoshikazu Masuhiro*†, Yoshihiro Mezaki*, Matomo Sakari*‡, Ken-ichi Takeyama*, Tasuku Yoshida*, Kunio Inoue§, Junn Yanagisawa*, Shigemasa Hanazawa†, Bert W. O'Malley¶, and Shigeaki Kato*‡‖

*Institute of Molecular and Cellular Biosciences, University of Tokyo, Bunkyo-ku, Tokyo 113-0032, Japan; †Division of Oral Infectious Diseases and Immunology, Faculty of Dental Science, Kyushu University, Higashi-ku, Fukuoka 812-8582, Japan; §Department of Biology, Faculty of Science, Kobe University, Nada-ku, Kobe 657-8501, Japan; ¶Department of Molecular and Cellular Biology, Baylor College of Medicine, Houston, TX 77030; and ‡Exploratory Research for Advanced Technology, Japan Science and Technology, Kawaguchi, Saitama 332-0012, Japan

Contributed by Bert W. O'Malley, April 19, 2005

Mitogen-activated protein kinase-mediated growth factor signals are known to augment the ligand-induced transactivation function of nuclear estrogen receptor α (ERα) through phosphorylation of Ser-118 within the ERα N-terminal transactivation (activation function-1) domain. We identified the spliceosome component splicing factor (SF)3a p120 as a coactivator specific for human ERα (hERα) activation function-1 that physically associated with ERα dependent on the phosphorylation state of Ser-118. SF3a p120 potentiated hERα-mediated RNA splicing, and notably, the potentiation of RNA splicing by SF3a p120 depended on hER Ser-118 phosphorylation. Thus, our findings suggest a mechanism by which growth factor signaling can regulate gene expression through the modulation of RNA splicing efficiency via phosphorylation of sequence-specific activators, after association between such activators and the spliceosome.

nuclear receptor | estrogen | coactivator | mitogen-activated protein kinase | RNA splicing

Most of the actions of estrogen are thought to be mediated via the transcriptional control of target genes by nuclear estrogen receptors (ER) α and β, members of the steroid hormone receptor gene superfamily that act as ligand-inducible transcription factors. ERs bind as dimers to specific estrogen response elements in the promoters of some target genes (1). However, most ER target promoters appear to recruit ERs without specific DNA binding, presumably through associations with sequence-specific factors bound to the promoters (2). ERs contain two transactivation functions (AFs), AF-1 in the N-terminal A/B domain and AF-2 in the C-terminal ligand-binding E/F domain. Ligand-induced transactivation by ERs requires multiple distinct classes of coactivator complexes, as well as a number of coregulators. The best-characterized complex contains p160/SRC family proteins (3, 4) and CBP/p300 histone acetyltransferases (5, 6), along with the RNA coactivator steroid receptor RNA activator (7) and presumably other known and unknown coactivators (8, 9). Another histone acetyltransferases-containing complex, the TBP-free TAF_{II}-containing (TFTC)-like complex (10), can also coactivate ER transactivation, as can the nonhistone acetyltransferases DRIP (VDR interacting protein)/TRAP (thyroid hormone receptor-associated protein)/SMCC (SRB/MED cofactor complexes)/ARC (activator-recruited cofactor) complex (11–13).

ER-mediated estrogen signaling is known to involve cross-talk with other signaling pathways (14). For instance, growth factors potentiate estrogen-induced cellular proliferation in female reproductive tissues (15). Phosphorylation of the Ser-118 residue in the human ERα (hERα) A/B domain by mitogen-activated protein kinase (MAPK) activated by growth factors (16, 17) and cyclin-dependent kinase-7 (18) results in the potentiation of AF-1 function (16). However, the molecular basis of ERα AF-1 potentiation by MAPK-mediated phosphorylation remains unclear. In a previous study, we identified the DEAD-box RNA helicase subfamily member p68/p72 as a hERα AF-1 coactivator that associated with steroid receptor RNA activator as a component in the p160/CBP histone acetyltransferases complex (19, 20). However, it appeared that the p68/p72-mediated facilitation of hERα AF-1 did not fully depend on Ser-118 phosphorylation, which suggested the presence of another, unknown factor. In the present study, we identified the spliceosome component splicing factor (SF)3a p120 as a coactivator specific for hERα AF-1 through Ser-118 phosphorylation-dependent interaction. Moreover, we found that this interaction potentiated hERα-mediated RNA splicing. Thus, our study indicated that MAPK-mediated cross-talk between growth factor and estrogen-signaling pathways modulates RNA splicing control through the phosphorylation-dependent interaction between hERα and a component of the spliceosome complex.

Materials and Methods

Plasmids and Constructs. The Pinpoint hERα (A/B) vector was prepared by inserting hERα (A/B) cDNA encoding amino acids 1–180 in-frame into HindIII/BamHI digested pinpoint Xa-3 vector (Promega). For Flag-SF3a p120 and Myc-SF3b p49 fusion constructs, respective cDNA fragments were amplified by PCR from a Marathon-Ready cDNA library (Clontech) by using pyrobest DNA polymerase (Takara, Tokyo). Myc-p68 and U1 70K cDNA were amplified by PCR, and the resultant products were digested and subcloned into pcDNA3-Flag (10), pcDNA3, and pCMV-Myc. pcDNA3-His-p72, pCMVβ-p300, pcDNA3-hERβ, pSG1-hERα, and mutants were as described (16, 20, 21). The complete coding sequences of all constructs used were verified by sequencing.

***In Vitro* Phosphorylation and Western Blotting of Biotin-Tagged hERα (A/B) Proteins.** Biotin-tagged hERα (A/B) and hERα (A/B)[S118A] proteins were expressed from Pinpoint Xa-3 vectors in *Escherichia coli* HB101, purified on avidin resin, and eluted with free biotin according to the manufacturer's protocol (Promega). To determine the efficiency of hERα (A/B) domain Ser-118 residue phosphorylation by MAPK *in vitro*, purified proteins and 50 ng of myelin basic protein (MBP) (Sigma) were coincubated for 30 min with MAPK (Erk2, New England Biolabs) in a total volume of 25 μl. Phosphorylated proteins were analyzed by 12.5% SDS/PAGE and autoradiography. Biotinylation of purified hERα (A/B) proteins was confirmed by Western blotting by using conjugated streptavidin-alkaline phosphatase (Promega).

Abbreviations: ERα, estrogen receptor α; hER, human ER; E2, 17β-estradiol; AF, transactivation function; TAM, 4-hydroxy-tamoxifen; SF, splicing factor; snRNP, small nuclear ribonucleoprotein particle; MAPK, mitogen-activated protein kinase; siRNA, short interfering RNA.

‖To whom correspondence should be addressed. E-mail: uskato@mail.ecc.u-tokyo.ac.jp.

www.pnas.org/cgi/doi/10.1073/pnas.0503197102

Far-Western Blotting and Expression Cloning. To detect endogenous interactants for phosphorylated Ser-118 hERα (A/B) domains, nuclear extracts from HeLa, COS-1, and MCF7 cells were prepared, and 10-μg aliquots of each nuclear extract were boiled and loaded onto 7.5% SDS/PAGE gels. Proteins were transferred onto poly(vinylidene difluoride) membranes and denatured in 6 M guanidine hydrochloride, 50 mM Tris·HCl (pH 8.0), 5 mM 2-mercaptoethanol, and 0.05% Tween 20 for 1 h at room temperature. Immobilized proteins were renatured overnight at 4°C. Membranes were rinsed and incubated with phosphorylated and biotin-tagged hERα (A/B) probe (0.1 μg/ml) for 4 h at room temperature. Membranes were washed and hybridization products detected by using conjugated streptavidin-alkaline phosphatase.

For expression cloning, a human kidney cDNA library in the Zap II vector was infected into bacteria, plated, and incubated at 42°C until minute plaques were seen. Recombinant plaques were grown at 37°C for 4 h and then induced with 1 mM isopropyl β-D-thiogalactoside-impregnated nitrocellulose filters for 3.5 h. Filters were then treated under the same conditions as for Far-Western blotting for denaturation and detection. Positive plaques were isolated, amplified, and processed, with the procedure repeated until 100% of the plaques were positive after plating. Four rounds of screening were performed after which cDNA inserts from plaques were obtained as pBluescript plasmids by *in vivo* excision. Isolated clones were sequenced by using T7 primers on an Applied Biosystems automatic sequencer.

Protein Identification by MALDI-TOF MS. Protein bands in SDS/PAGE gels were excised and digested in-gel with trypsin. Eluted peptides were then loaded onto the sampling plate for MALDI-TOF MS (Voyager DE-STR, Perseptive Biosystems). After analysis of each protein fragment mass, results were compared by using the MS-FIT program (University of California, San Francisco Mass Spectrometry Facility).

Pull-Down Assay. GST-fused proteins were expressed in *E. coli* and purified on glutathione-Sepharose beads (Amersham Pharmacia). Pull-down assays were performed as described (10, 16, 19–21). Immobilized glutathione-Sepharose and avidin-resin were incubated with ^{35}S-methionine-labeled SF3a p120 protein. Bound proteins were eluted and analyzed by 7.5% SDS/PAGE.

Splicing Assay. The 293T cells were transfected with reporter CD44 minigene (22), pCH110 internal control plasmid containing β-galactosidase (10 ng), short-interfering RNA (siRNA), and expression plasmids as indicated. Total RNA was isolated by Isogen (Nippon Gene, Toyama, Japan), and RT-PCR for CD44 was performed as described (22). For oxytocin, total RNA (0.1 μg) was reverse-transcribed in 50-μl reaction mixtures by using the Access RT-PCR system (Promega) with primers specific for oxytocin (reverse, 5′-CAGGTAGTTCTCCTCCTGGCAGC-3′) or β-galactosidase (reverse, 5′-CCGCCGATACTGACGGGCTCC-3′). PCR was then performed by using 3 μl of this mixture in a 50-μl reaction volume containing 0.5 unit of ExTaqDNA polymerase (Takara) and gene-specific primers for oxytocin (forward, 5′-CAGCCTCGCTTGCTGTCTGCTC-3′; reverse, 5′-CAGGTAGTTCTCCTCCTGGCAGC-3′) or β-galactosidase (forward, 5′-CGACCGCTCACGCGTGGCAGC-3′; reverse, 5′-CCGCCGATACTGACGGGCTCC-3′). PCR conditions were optimized to allow semiquantitative measurement of oxytocin (denaturation at 96°C for 1 min followed by 25–30 cycles of 96°C for 20 s, 70°C for 20 s, and 72°C for 1 min) and β-galactosidase (denaturation at 96°C for 1 min followed by 20–25 cycles of 96°C for 20 s, 70°C for 20 s, and 72°C for 1 min) mRNA levels. PCR products were verified by sequencing and visualized on 2% agarose/Tris-acetate-EDTA gels. Quantitative measurement of splicing efficiency was analyzed by NIH IMAGE (National Institutes of Health, Bethesda).

Chromatin Immunoprecipitation Assay. Chromatin immunoprecipitation assays for oxytocin were performed as described (10, 23). Soluble chromatin from MCF7 cells was immunoprecipitated with Abs against the indicated proteins. Specific primer pairs used to PCR amplify oxytocin were 5′-CACCCTAGTGGCCCAGGCCACC-3′ and 5′-GCTCTGTTTAAGAGGTTGGTAGTATG-3′. PCR conditions were optimized to allow semiquantitative measurement. Conditions used were 21–25 cycles of 20 s at 96°C, 20 s at 70°C, and 1 min at 72°C. PCR products were visualized on 2% agarose/Tris-acetate-EDTA gels.

Results and Discussion

Identification of SF3a p120 as a Direct Interactant for hERα Phosphorylated by MAPK at Ser-118. To identify the factor fully responsible for the phosphorylation-dependent potentiation of hERα AF-1, we performed Far-Western blot analysis on nuclear extracts by using bacterially expressed biotinylated hERα (A/B) domains as a probe. hERα (A/B) domains, phosphorylated *in vitro* by MAPK, detected three endogenous proteins with approximate M_r of 120, 72, and 68 kDa in nuclear extracts from the HeLa, COS-1, and MCF7 cell lines (Fig. 1*A Center*, lanes 5–7). As the 68- and 72-kDa bands corresponded to p68/p72 (19, 20) by Western blotting with specific Abs (data not shown), we attempted to clone the p120 factor by Far-Western screening of a human kidney cDNA library because ERα AF-1 activity is high in the kidney. Screening of 8×10^6 independent clones yielded 72 positives, three of which encoded overlapping cDNA sequences that corresponded to the C-terminal domain of SF3a p120 (24, 25). Biochemical purification of interactants from stably expressed hERα (Fig. 1*B Right*) and phosphorylated hERα A/B domains fused to GST [GST-*p*-Ser-118 hERα (A/B)] (Fig. 1*B Left*, lane 5) followed by MS (MALDI-TOF MS) confirmed the identity of the three isolated proteins as SF3a p120 and p68/p72. No such association was detected by using a hERα mutant that cannot be phosphorylated by MAPK because of the substitution of the Ser-118 residue with Ala [S118A (16) (Fig. 1*B*, *Right*)].

We then tested whether SF3a p120 directly bound the A/B or E/F domains of hERα or hERβ by using an *in vitro* GST pull-down assay (10). Unlike p68/p72 (19, 20), SF3a p120 exhibited a strict association only with A/B domains from phosphorylated Ser-118 hERα and Glu-118 hERα (S118E), a transcriptionally dominant active mutant with Ser-118 substituted with Glu to mimic the negative charge of phosphorylated Ser-118 (Fig. 1*C*, lanes 4 and 5). In contrast, SF3a p120 did not interact with the Ser-118–Ala mutant (Fig. 1*C*, lane 3), the E/F domain of ERα, or ERβ A/B or D/E/F domains (see Fig. 1*C*, lanes 7–11). We then tested whether SF3a p120 directly associated with hERα *in vivo* by using immunoprecipitation assays on 293T cells. The *in vivo* association between SF3a p120 and full-length hERα depended on ligand binding and was abrogated by both the MAPK inhibitor U0126 (Fig. 2*A*, compare lanes 6 and 7) and the Ser-118–Ala mutant (Fig. 2*A*, lanes 8–10). As expected from the coimmunoprecipitation assay results (Fig. 2*A*), activation of MAPK signaling by EGF treatment potentiated the association of hERα with endogenous SF3a p120 in MCF7 cells (Fig. 2*B*, lane 3). As the hERα AF-1 domain (hERα A/B/C) alone appeared to be sufficient for association with SF3a p120 (Fig. 2*A*, lane 12), it is possible that the structural alterations in ERα induced by ligand binding expose the functional AF-1 domain, rendering it accessible to SF3a p120.

SF3a p120 Is a Coactivator for Ser-118 Phosphorylated hERα AF-1. As SF3a p120 appeared to physically interact with the hERα AF-1 domain, we tested the coregulatory function of SF3a p120 in a

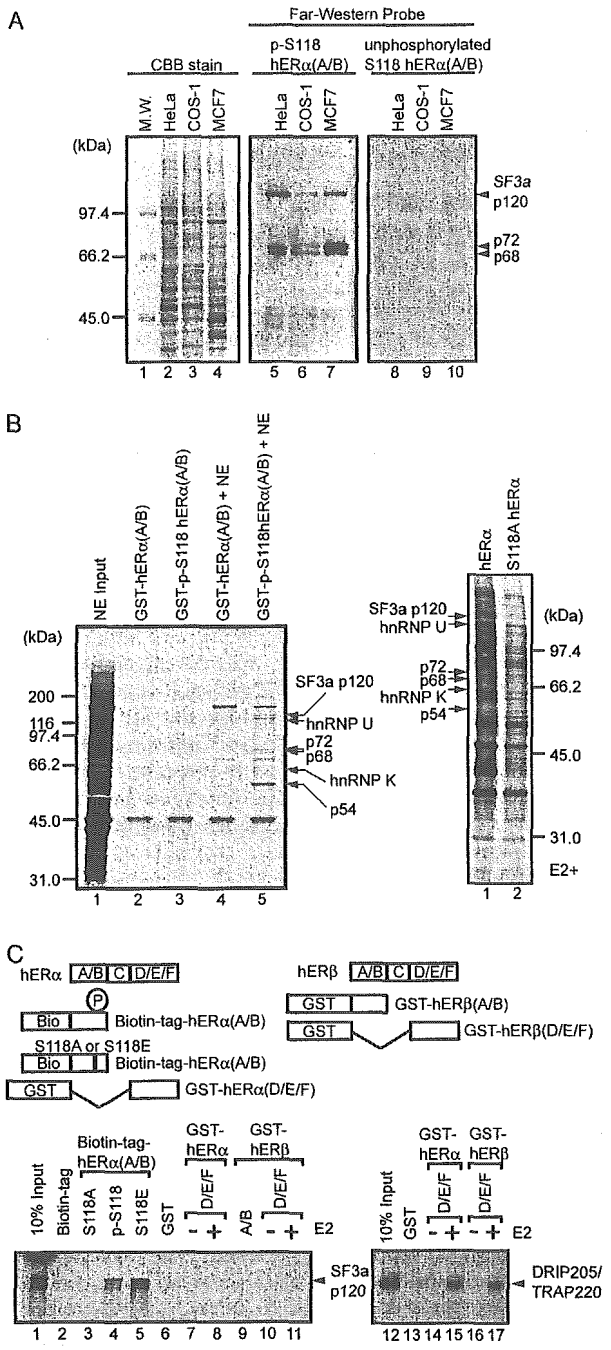

Fig. 1. *SF3a p120 directly binds phosphorylated Ser-118 hERα (A/B) domains.* (*A*) Endogenous interactants of the hERα (A/B) domain. Three endogenous interactants (p120, p72, and p68, as indicated) were detected in 10 μg of nuclear extracts from HeLa, COS-1, and MCF7 cells lines with Ser-118 phosphorylated or nonphosphorylated hERα (A/B) domain probes by using the Far-Western technique (20). (*Left*) Coomassie brilliant blue R-250 (CBB)-stained gel. (*B*) Identification of phosphorylated hERα (A/B) domain-interacting proteins. Nuclear extracts prepared from HeLa S3 cells were incubated with immobilized GST-hERα (A/B) or GST-*p*-Ser-118 hERα (A/B) domains. (*Left*) Proteins eluted from the columns by 1 M KCl were subjected to SDS/PAGE followed by staining with CBB. (*Right*) Products of FLAG-M2 resin affinity purification from nuclear extracts of HeLa cells stably expressing FLAG-hERα or FLAG-Ser-118–Ala hERα were examined by MS. Identified proteins are indicated at the right. (*C*) Selective binding of SF3a p120 to hERα in a pull-down assay. *In vitro*-translated SF3a p120 protein was tested for direct interaction with biotin-tagged hERα (A/B), chimeric GST-fused A/B domain of hERβ, or D/E/F domains of hERα or hERβ. DRIP205/TRAP220 was used as a positive control and exhibited ligand-induced association with the hERα D/E/F domain.

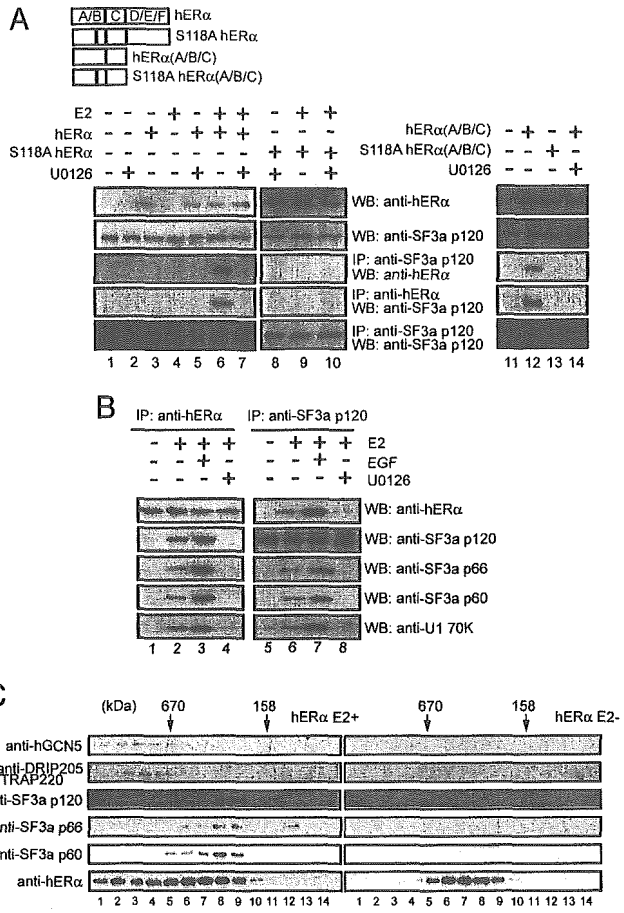

Fig. 2. Association of hERα AF-1 domain with spliceosome complex through SF3a p120. (*A*) *In vivo* association of hERα and SF3a p120. The 293T cells were transfected with hERα expression vectors (0.1 μg) and then incubated with or without E2 (10^{-8} M). Cells were then lysed in TNE buffer (10 mM Tris·HCl, pH 7.5, 150 mM NaCl, 1 mM EDTA, 1% NP-40) and immunoprecipitated with anti-hERα or anti-Flag SF3a p120 Ab. Immunoprecipitates were subjected to SDS/PAGE followed by Western blotting with the indicated Abs. (*B*) Ligand-induced association of full-length hERα with U1/U2 components was further characterized by using endogenous proteins in MCF7 cells. Cells were treated with E2 (10–8 M), EGF (100 ng/ml), and MAPK inhibitor U0126 (20 μM), as indicated, and then immunoprecipitated with anti-hERα or anti-SF3a p120 Ab. Immunoprecipitates were subjected to SDS/PAGE followed by Western blotting with the indicated Abs. (*C*) hERα associates with a complex containing SF3a spliceosome components. Nuclear extracts from a stable transformant of FLAG-tagged full-length hERα with or without E2 (10^{-7} M) were applied to FLAG-M2 resin, and eluted proteins were separated by using Superose 6 gel filtration column (10, 14) and detected by the indicated Abs.

transient transfection experiment by using a luciferase reporter plasmid bearing estrogen response elements (10, 20) transfected into 293T cells. Although SF3a p120 enhanced the estrogen-induced transactivation function of full-length hERα (Fig. 3*A*, lane 5), with a 2- to 3-fold increase in hERα (A/B/C) AF-1 activity (Fig. 3*B*, lane 5), no potentiation of AF-2 activity of hERα (D/E/F) was observed (data not shown). Introduction of SF3a p120 siRNA significantly lowered the ligand-induced transactivation of hERα and dramatically attenuated MAPK signaling-induced potentiation (Fig. 3*A*, lanes 6, 9, and 12). To examine the AF-1-specific coactivator function of SF3a p120 for full-length hERα, we tested SF3a p120 activity on hERα bound to 4-hydroxy-tamoxifen (TAM), an AF-1 agonist/AF-2 antagonist (16). As expected, partial transactivation of TAM-bound ERα was observed, presumably via activated AF-1 (Fig. 3*A*, lanes 19–27). This transactivation was potentiated by both SF3a p120

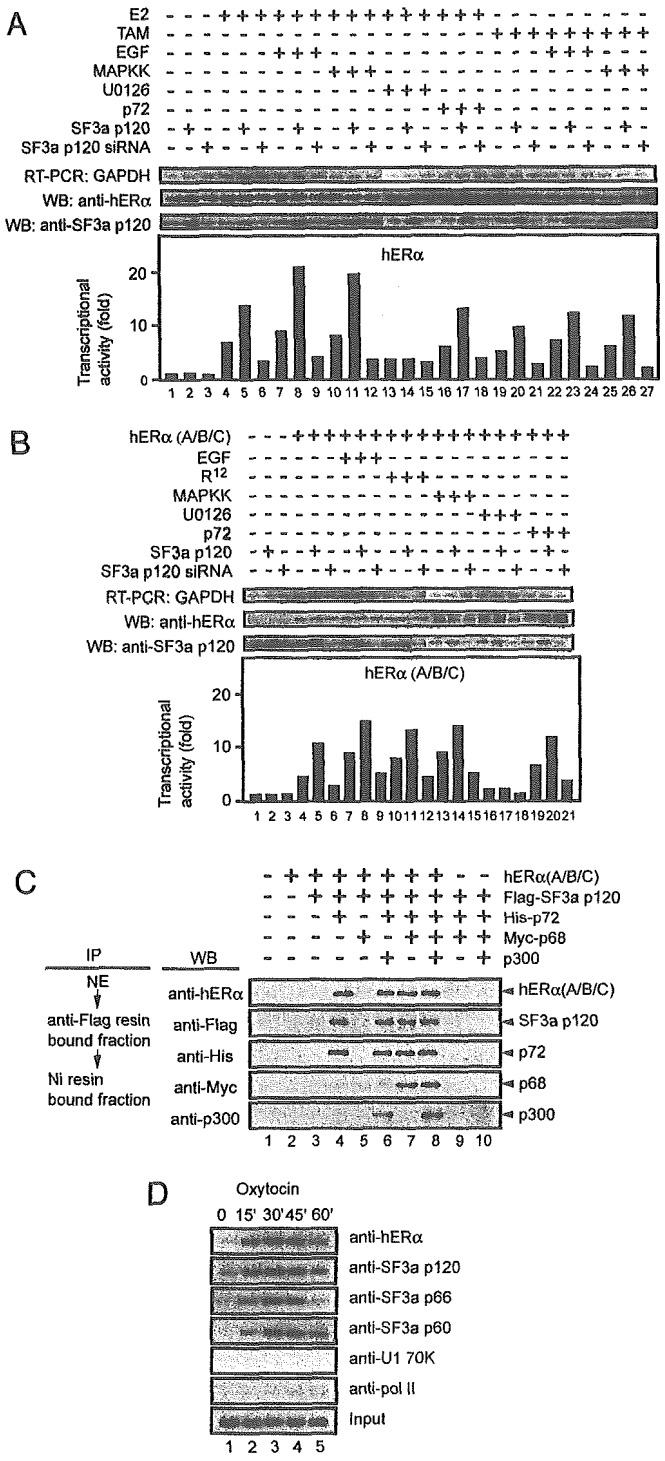

Fig. 3. SF3a p120 coactivates the transactivation function of hERα AF-1. (*A* and *B*) SF3a p120 potentiates the transactivation function of hERα AF-1 in a Ser-118 phosphorylation-dependent manner. The 293T cells were transfected with expression vectors of full-length hERα (50 ng), hERα (A/B/C) (50 ng), Ki-Ras^{val12} (R^{12}) (100 ng), MAPKK (100 ng), SF3a p120 (300 ng), or combinations as indicated, in either the absence or presence of E2 (10^{-8} M), TAM (10^{-7} M), U0126 (20 μM), or combinations as indicated, along with pGL-estrogen response element-tk (1.0 μg) and pRL-CMV (10 ng). Cultured cells were also transfected with 100 pmol dsRNA for SF3a p120 siRNA (5′-AGACGGAAUGGAAACUGAAUGGGCAAG-3′ and 5′-UGCCCAUUCAGUUUCCAUUCCGUCUAU-3′) by using Lipofectamine 2000 (Invitrogen). Assays were performed 24 h after transfection. (*Upper*) Cell extracts were used in luciferase assays (20) and Western blotting. (*C*) SF3a p120 enhances the association of hERα AF-1 with p68, p72, and p300. The 293T cells were transfected with indicated plasmids. The complex associated with A/B/C domains of hERα were analyzed to detect SF3a p120, p68, p72, and p300 by purification from the cell extracts with anti-Flag M2 resin and Ni resin, followed by Western blotting by using the anti-hERα, anti-Flag, anti-His, anti-Myc, or anti-p300 Abs (lanes 1–10). (*D*) Occupancy of human oxytocin promoter by hERα and spliceosome components in MCF7 cells was determined by chromatin immunoprecipitation analysis (14, 23).

and MAPK activators, with the simultaneous addition of MAPK activators and SF3a p120 resulting in additive potentiation (Fig. 3*A*, compare lane 19 and lanes 20, 23, and 26). To further examine the SF3a p120 hERα AF-1 coactivator function, possible interaction with known hERα AF-1 coactivators was tested by coimmunoprecipitation by using SF3a p120. p68/p72 and p300 were detected in the SF3a p120 coimmunoprecipitants (data not shown), and we then verified these associations by further testing the complexes that formed around the hERα AF-1 domain (Fig. 3*C*). Purification of the SF3a p120-containing complex that associated with hERα (A/B/C) by using sequential affinity columns identified p68/72 and p300, which raised the hypothesis that SF3a p120 was the associating component of the p68/72 and p300 hERα AF-1 coactivator complex (20).

To examine these *in vivo* associations, we performed a chromatin immunoprecipitation assay by using full-length hERα in MCF7 cells, spliceosome complex components, and a gene promoter region from human oxytocin that contained an estrogen-responsive element (26). Upon 17β-estradiol (E2) stimulation, the SF3a subunits and hERα all were recruited to the oxytocin promoter along with RNA polymerase II (Fig. 3*D*).

Phosphorylated hERα Associates with the Spliceosome Through SF3a p120. Because SF3a p120 is known to be a component of U2 small nuclear ribonucleoprotein particle, which forms the spliceosome along with the U1 complex (24, 25), we used coimmunoprecipitation to determine whether phosphorylated hERα associated with the spliceosome via SF3a p120. Coimmunoprecipitation experiments were performed with extracts from hERα-expressing MCF7 cells, and results indicated that all U1/U2 endogenous components tested (U2: SF3a p66, SF3a p60 small nuclear ribonucleoprotein particles; and U1: U1 70K small nuclear ribonucleoprotein particles) (27, 28) were coimmunoprecipitated with endogenous hERα, with these associations potentiated by EGF treatment (Fig. 2*B*, lanes 1–4). Similar results were obtained by using anti-SF3a p120 (Fig. 2*B*, lanes 5–8). Moreover, the U2 components were detected as a single complex by Western blotting after liganded hERα-associated complexes were biochemically isolated from HeLa nuclear extracts and fractionated by gel filtration (10, 14, 29) (Fig. 2*C Left*, lanes 8 and 9).

SF3a p120 Potentiates hERα-Mediated RNA Splicing. To test whether the phosphorylation-dependent association of hERα with spliceosome components modulated mRNA processing, we examined the effect of SF3a p120 on RNA splicing by using a test CD44 minigene, as reported (Fig. 4*A*) (22). Although estrogen (E2) stimulated transcription via hERα or hERβ (Fig. 4*B*, lanes 6 and 12), the ratio of skipped to unskipped transcripts was enhanced only by liganded ERα. SF3a p120 clearly potentiated hERα-mediated RNA splicing (Fig. 4*B*, lane 7). Unlike SF3a p120, neither p68 nor p72 was able to potentiate intron excision. Indeed, p68/p72 inhibited exon skipping in the CD44 minigene (Fig. 4*B*, lane 8), as expected from previous studies (22, 30), despite the finding that p68/p72 coactivated ERα-mediated transcription (see Fig. 3*A*, lane 16–18, for p72 activity as a representative of p68/p72) (19, 20). Similar results were observed by using a human β-globin minigene and a mutant ERα AF-1 domain fused to the yeast GAL4-DNA binding domain. In

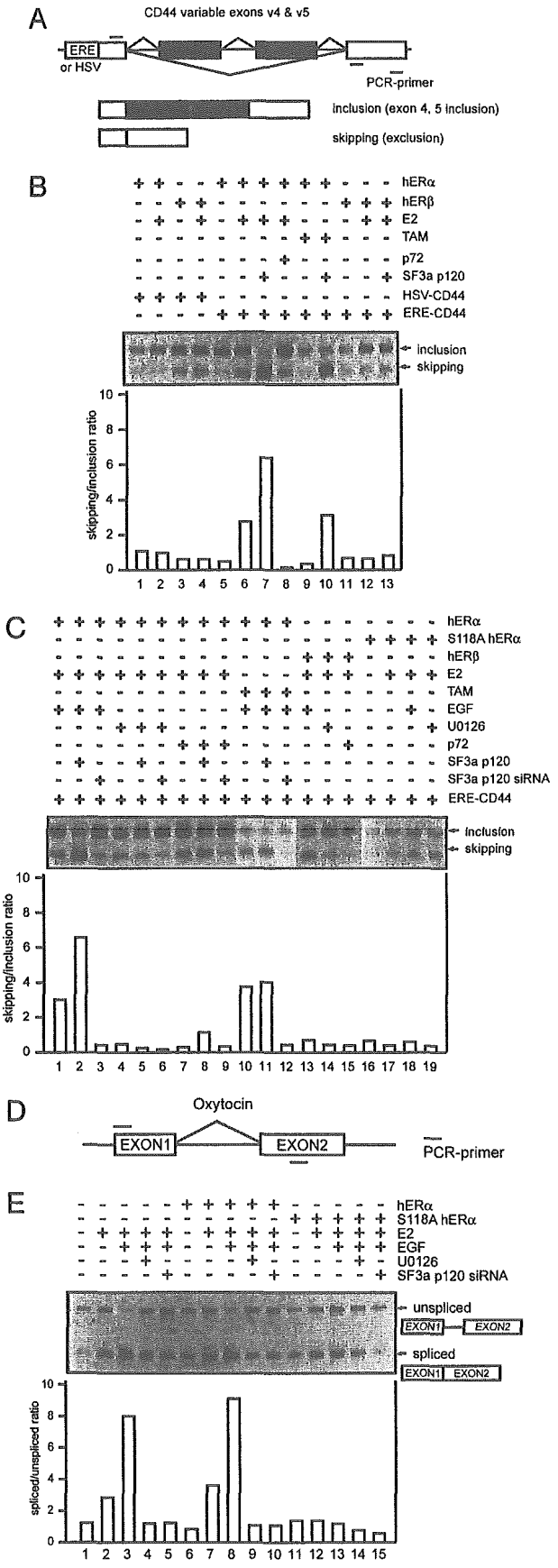

Fig. 4. hERα AF-1-specific potentiation of mRNA processing by SF3a p120. (*A*) Schematic representation of the estrogen response element-CD44 construct used in the *in vivo* splicing assay (22). (*B* and *C*) SF3a p120 regulation of CD44 mRNA processing depends on hERα Ser-118 phosphorylation state. The 293T cells were transfected with the indicated plasmids and siRNA (SF3a p120; 100 pmol). After transfection, cells were treated with E2 (10−8 M), TAM (10−7 M), EGF (100 ng/ml), and U0126 (20 μM) as indicated. Total RNA was extracted with Isogen 24 h after transfection and subjected to RT-PCR analysis (22). (*D*) Schematic representation of the human oxytocin gene exon 1 and 2 used in the *in vivo* splicing assay. (*E*) MCF7 cells were transfected with the indicated plasmids and treated as in *B* and *C*. After the treatment, total RNA was extracted. Splicing patterns were evaluated by RT-PCR by using oxytocin-specific primers.

that system, the hERα AF-1 domain alone was able to potentiate RNA splicing (data not shown).

RNA Splicing Augmented by hERα Depends on hERα Ser-118 Phosphorylation by MAPK. Reflecting the Ser-118 phosphorylation-dependent association between hERα and SF3a p120 (Fig. 2*A*), both Ala substitution in the AF-1 domain (S118A) (Fig. 4*C*, lanes 16–19) and SF3a p120 siRNA (Fig. 4*C*, lanes 3, 6, and 9) abrogated the potentiation of intron excision by hERα. The efficiency of RNA splicing from the CD44 minigene mediated by hERα appeared to depend on SF3a p120 expression level and activated MAPK signaling via EGF treatment (Fig. 4*C*, compare lanes 1 and 4). TAM treatment (20) further confirmed the AF-1 specificity of SF3a p120 on hERα (Fig. 4*B*, compare lanes 9 and 10). Neither potentiation of exon skipping by SF3a p120 nor increased RNA splicing caused by activated MAPK was observed for the full-length hERα Ser-118–Ala mutant (Fig. 4*C*, lanes 16–19). Reflecting the phosphorylation-dependent association of SF3a p120 with hERα through the A/B AF-1 domain, activation of MAPK by Ki-Ras^{val12}, MAPKK, or EGF also potentiated the effects of SF3a p120 on RNA splicing mediated by the hERα A/B-AF-1 domain alone (data not shown). Such potentiation via activated MAPK signaling was not detectable in the hERα Ser-118–Ala mutant A/β-GAL-DNA binding domain (data not shown). Notably, neither a significant increase in spliced transcript stability nor specific intracellular localization was observed when transcription was potentiated under any of the conditions tested (data not shown).

Finally, to address the physiological relevance of our findings, we screened several known endogenous ERα target genes that show ERα-regulated splicing. We found that the human oxytocin gene generated a transcript that retained intron 1 sequence (see Fig. 4*D*). In response to E2 treatment, intron 1 splicing was increased along with enhanced transcription in MCF7 cells (Fig. 4*E*, compare lanes 1 and 2). EGF-mediated MAPK activation further enhanced RNA splicing mediated by hERα (Fig. 4*E*, lanes 3 and 8). However, Ser-118–Ala hERα expression abrogated this increase in RNA splicing after EGF treatment (Fig. 4*E*, lane 13). Thus, our findings suggested that the potentiation of splicing efficiency mediated via the association of phosphorylated hERα with SF3a p120 occurred in at least some hERα target genes.

Cross-Talk Between Estrogen and Growth Factor Signaling Mediates the Control of RNA Splicing. Our study uncovered a unique mechanism by which RNA splicing is potentiated by MAPK-mediated growth factor signaling through Ser-118 phosphorylation of hERα, such that augmented RNA splicing may, at least in part, account for the effects of SF3a p120 coactivation on the ligand-induced transactivation functions of hERα. Based on our findings, it is also possible that phosphorylated, but DNA-unbound, hERα may serve as a coregulator of RNA splicing in some estrogen-responsive gene promoters. Recent reports have shown that the RNA splicing process is coupled with transcriptional events under the control of sequence-specific activators, such as peroxisome proliferator-activated

receptor (PPAR)γ and steroid receptors (22, 30–35). Thus, given the current view that the progression from transcription to splicing is a sequential, yet rapid process (36), it is likely that the spliceosome functionally associates, directly or indirectly, with activator molecules, presumably including coregulators and transcription elongation factors. The efficiency of RNA splicing is then modulated via the association between transcription-related factors and the spliceosome. The present study provides an example of coordinated regulation of transcription and intron excision modulated by growth factor signaling via the association of an activator with the spliceosome. This mechanism may support, at least in part, growth factor-mediated gene regulation.

We thank Dr. C. Will (Max Planck Institute, Gottingen, Germany) for the kind gift of the U1 70K plasmid; Drs. M. Saitoh, K. Goto, and H. Nawata for technical help; Drs. P. Chambon, D. Metzger, and H. Kawate for helpful suggestions and plasmids; and H. Higuchi for manuscript preparation. This work was supported in part by the Program for Promotion of Basic Research Activities for Innovative Biosciences and priority areas from the Ministry of Education, Science, Sports and Culture of Japan (to S.K.) and National Institutes of Health Grant 08818 (to B.W.O.).

1. Parker, M. G. (1998) *Biochem. Soc. Symp.* **63,** 45–50.
2. Kushner, P. J., Agard, D. A., Greene, G. L., Scanlan, T. S., Shiau, A. K., Uht, R. M. & Webb, P. (2000) *J. Steroid Biochem. Mol. Biol.* **74,** 311–317.
3. Onate, S. A., Tsai, S. Y., Tsai, M. J. & O'Malley, B. W. (1995) *Science* **270,** 1354–1357.
4. Chen, H., Lin, R. J., Schiltz, R. L., Chakravarti, D., Nash, A., Nagy, L., Privalsky, M. L., Nakatani, Y. & Evans, R. M. (1997) *Cell* **90,** 569–580.
5. Kamei, Y., Xu, L., Heinzel, T., Torchia, J., Kurokawa, R., Gloss, B., Lin, S. C., Heyman, R. A., Rose, D. W., Glass, C. K., *et al.* (1996) *Cell* **85,** 403–414.
6. Spencer, T. E., Jenster, G., Burcin, M. M., Allis, C. D., Zhou, J., Mizzen, C. A., McKenna, N. J., Onate, S. A., Tsai, S. Y., Tsai, M. J., *et al.* (1997) *Nature* **389,** 194–198.
7. Lanz, R. B., McKenna, N. J., Onate, S. A., Albrecht, U., Wong, J., Tsai, S. Y., Tsai, M. J. & O'Malley, B. W. (1999) *Cell* **97,** 17–27.
8. McKenna, N. J. & O'Malley, B. W. (2002) *Cell* **108,** 465–474.
9. Spiegelman, B. M. & Heinrich, R. (2004) *Cell* **119,** 157–167.
10. Yanagisawa, J., Kitagawa, H., Yanagida, M., Wada, O., Ogawa, S., Nakagomi, M., Oishi, H., Yamamoto, Y., Nagasawa, H., McMahon, S. B., *et al.* (2002) *Mol. Cell* **9,** 553–562.
11. Fondell, J. D., Ge, H. & Roeder, R. G. (1996) *Proc. Natl. Acad. Sci. USA* **93,** 8329–8333.
12. Rachez, C., Lemon, B. D., Suldan, Z., Bromleigh, V., Gamble, M., Naar, A. M., Erdjument-Bromage, H., Tempst, P. & Freedman, L. P. (1999) *Nature* **398,** 824–828.
13. Naar, A. M., Beaurang, P. A., Zhou, S., Abraham, S., Solomon, W. & Tjian, R. (1999) *Nature* **398,** 828–832.
14. Ohtake, F., Takeyama, K., Matsumoto, T., Kitagawa, H., Yamamoto, Y., Nohara, K., Tohyama, C., Krust, A., Mimura, J., Chambon, P., *et al.* (2003) *Nature* **423,** 545–550.
15. Couse, J. F. & Korach, K. S. (1999) *Endocr. Rev.* **20,** 358–417.
16. Kato, S., Endoh, H., Masuhiro, Y., Kitamoto, T., Uchiyama, S., Sasaki, H., Masushige, S., Gotoh, Y., Nishida, E., Kawashima, H., *et al.* (1995) *Science* **270,** 1491–1494.
17. Feng, W., Webb, P., Nguyen, P., Liu, X., Li, J., Karin, M. & Kushner, P. J. (2001) *Mol. Endocrinol.* **15,** 32–45.
18. Chen, D., Riedl, T., Washbrook, E., Pace, P. E., Coombes, R. C., Egly, J. M. & Ali, S. (2000) *Mol. Cell* **6,** 127–137.
19. Endoh, H., Maruyama, K., Masuhiro, Y., Kobayashi, Y., Goto, M., Tai, H., Yanagisawa, J., Metzger, D., Hashimoto, S. & Kato, S. (1999) *Mol. Cell. Biol.* **19,** 5363–5372.
20. Watanabe, M., Yanagisawa, J., Kitagawa, H., Takeyama, K., Ogawa, S., Arao, Y., Suzawa, M., Kobayashi, Y., Yano, T., Yoshikawa, H., *et al.* (2001) *EMBO J.* **20,** 1341–1352.
21. Kobayashi, Y., Kitamoto, T., Masuhiro, Y., Watanabe, M., Kase, T., Metzger, D., Yanagisawa, J. & Kato, S. (2000) *J. Biol. Chem.* **275,** 15645–15651.
22. Auboeuf, D., Honig, A., Berget, S. M. & O'Malley, B. W. (2002) *Science* **298,** 416–419.
23. Shang, Y., Hu, X., DiRenzo, J., Lazar, M. A. & Brown, M. (2000) *Cell* **103,** 843–852.
24. Brosi, R., Groning, K., Behrens, S. E., Luhrmann, R. & Kramer, A. (1993) *Science* **262,** 102–105.
25. Brosi, R., Hauri, H. P. & Kramer, A. (1993) *J. Biol. Chem.* **268,** 17640–17646.
26. Stedronsky, K., Telgmann, R., Tillmann, G., Walther, N. & Ivell, R. (2002) *J. Neuroendocrinol.* **14,** 472–485.
27. Nilsen, T. W. (2003) *BioEssays* **25,** 1147–1149.
28. Soret, J. & Tazi, J. (2003) *Prog. Mol. Subcell. Biol.* **31,** 89–126.
29. Kitagawa, H., Fujiki, R., Yoshimura, K., Mezaki, Y., Uematsu, Y., Matsui, D., Ogawa, S., Unno, K., Okubo, M., Tokita, A., *et al.* (2003) *Cell* **113,** 905–917.
30. Cramer, P., Caceres, J. F., Cazalla, D., Kadener, S., Muro, A. F., Baralle, F. E. & Kornblihtt, A. R. (1999) *Mol. Cell* **4,** 251–258.
31. Monsalve, M., Wu, Z., Adelmant, G., Puigserver, P., Fan, M. & Spiegelman, B. M. (2000) *Mol. Cell* **6,** 307–316.
32. Iwasaki, T., Chin, W. W. & Ko, L. (2001) *J. Biol. Chem.* **276,** 33375–33383.
33. Zhao, Y., Goto, K., Saitoh, M., Yanase, T., Nomura, M., Okabe, T., Takayanagi, R. & Nawata, H. (2002) *J. Biol. Chem.* **277,** 30031–30039.
34. Brand, M., Moggs, J. G., Oulad-Abdelghani, M., Lejeune, F., Dilworth, F. J., Stevenin, J., Almouzni, G. & Tora, L. (2001) *EMBO J.* **20,** 3187–3196.
35. Honig, A., Auboeuf, D., Parker, M. M., O'Malley, B. W. & Berget, S. M. (2002) *Mol. Cell. Biol.* **22,** 5698–5707.
36. Orphanides, G. & Reinberg, D. (2002) *Cell* **108,** 439–451.

0022-3565/05/3152-545–552$20.00
THE JOURNAL OF PHARMACOLOGY AND EXPERIMENTAL THERAPEUTICS
Copyright © 2005 by The American Society for Pharmacology and Experimental Therapeutics
JPET 315:545–552, 2005

Vol. 315, No. 2
87643/3057203
Printed in U.S.A.

Human Expanded Polyglutamine Androgen Receptor Mutants in Neurodegeneration as a Novel Ligand Target

Takashi Furutani, Ken-ichi Takeyama, Masahiko Tanabe, Hiroshi Koutoku, Saya Ito, Nobuaki Taniguchi, Eriko Suzuki, Masafumi Kudoh, Masayuki Shibasaki, Hisataka Shikama, and Shigeaki Kato

Drug Discovery Research, Astellas Pharma Inc., Tsukuba, Japan (T.F., H.K., N.T., M.K., M.S., H.S.); Institute of Molecular and Cellular Biosciences, The University of Tokyo, Tokyo, Japan (K.-I.T., M.T., S.I., E.S., S.K.); and Exploratory Research for Advanced Technology, Japan Science and Technology, Kawaguchi, Saitama, Japan (S.K.)

Received April 7, 2005; accepted July 15, 2005

ABSTRACT

Androgen receptor (AR) plays key roles in various biological events, including pathological processes such as prostate cancer, androgen-insensitive syndrome, and spinal and bulbar muscular atrophy (SBMA). SBMA is caused by mutation of the expanded polyglutamine (polyQ) stretches in the AR gene. Recently, we established a *Drosophila* SBMA model that expresses the expanded polyQ hAR mutant in eyes, which monitors neurodegeneration as a rough eye phenotype. In addition, we showed that androgen binding to the mutant hAR causes structural alterations, leading to the onset of neurodegeneration in the fly eyes. In the present study, we examined whether the ligand-induced neurodegeneration via the hAR mutant is coupled with the known ligand-induced transactivation function of hAR. By testing several known AR antagonists and several of their structure-related compounds, we unexpectedly found that none of the AR ligands antagonized the hAR mutant neurodegeneration function, and surprisingly, compound 4-(4,4-dimethyl-2,5-dioxo-1-imidazolidinyl)-2-trifluoromethylbenzonitrile (RU56279) was more potent in inducing neurodegeneration. However, in vitro and in vivo mammalian assays showed that RU56279 exhibited the expected antagonistic activity with the same potency as those of the other compounds. Thus, these findings suggest the presence of a novel ligand-induced function of the polyQ hAR mutant in neurodegeneration that could not be prevented by known antagonists for the hAR transactivation function.

Androgen plays pivotal roles in male reproductive organs and sexual behaviors (Mooradian et al., 1987; Wilson, 1999) and is also well known to be deeply involved in pathophysiological events like androgen-dependent prostate cancer development and androgen-induced onset of spinal and bulbar muscular atrophy (SBMA), a rare degenerative disease of motor neurons characterized by progressive muscle atrophy and weakness in male patients usually beginning at 30 to 50 years of age (La Spada et al., 1991; Choong and Wilson, 1998; Merry and Fischbeck, 1998). Such androgen actions in physiological and pathophysiological events are considered to mediate gene regulation by the nuclear androgen receptor (AR). Mapping studies and functional analyses of SBMA cases revealed expansions in the number of trinucleotide CAG repeats in the first exon of the AR gene, which generate expanded polyglutamine (polyQ) stretches in the N-terminal A/B domain of the hAR protein. Disease onset occurs when the stretches contain more than 40 glutamine residues, compared with a range of 8 to 34 glutamine residues in normal individuals (La Spada et al., 1991; Merry and Fischbeck, 1998).

AR is a member of the nuclear receptor (NR) superfamily and acts as a ligand-inducible transcription factor (Mangelsdorf et al., 1995; Glass and Rosenfeld, 2000). Members of the nuclear receptor superfamily share common structural features with distinct functional domains, referred to as domains A to E/F. The highly conserved middle region (C domain) acts as a DNA binding domain (DBD), whereas the ligand binding domain

This work was supported by a grant-in-aid for Scientific Research (S.K.) and Scientific Research on Priority Areas (S.K.) from the Minister of Education, Science and Culture, Tokyo, Japan.
Article, publication date, and citation information can be found at http://jpet.aspetjournals.org.
doi:10.1124/jpet.105.087643.

ABBREVIATIONS: SBMA, spinal and bulbar muscular atrophy; AR, androgen receptor; polyQ, polyglutamine; hAR, human AR; NR, nuclear receptor; DBD, DNA binding domain; LBD, ligand binding domain; AF, autonomous activation function; RU, 4-(4,4-dimethyl-2,5-dioxo-1-imidazolidinyl)-2-trifluoromethylbenzonitrile (RU56279); DHT, dihydrotestosterone; HF, hydroxyflutamide; BIC, bicalutamide; NIL, nilutamide; GFP, green fluorescent protein; UAS, upstream activating sequence; LM, light microscope; SEM, scanning electron microscope; DMSO, dimethyl sulfoxide; CHO, Chinese hamster ovary; GST, glutathione *S*-transferase; ARE, androgen response element; GMR, glass multimer receptor; wt, wild type; MMTV, mouse mammary tumor virus.

(LBD) is located in the less well conserved C-terminal E/F domain. The LBDs of most nuclear receptors, including AR, have been analyzed and have been shown to consist of 12 α-helices that form a pocket to capture cognate ligands (Shiau et al., 1998; Poujol et al., 2000). The autonomous activation function-1 (AF-1) within the A/B domain is ligand-independent, whereas the AF-2 in the LBD is induced upon ligand binding (Kato et al., 1995). Ligand-free LBD appears to suppress the function of AF-1, although ligand binding to the LBD is thought to evoke the function of LBD and to restore the A/B domain function through a yet undescribed intramolecular alteration of the entire receptor structure. During ligand-induced transcriptional controls, AF-1 and AF-2 act as interacting regions for the coregulators (He et al., 1999; Watanabe et al., 2001; Shang et al., 2002). Upon ligand binding, the most C-terminal α-helix 12 (H12) in the LBD shifts position to create a space, with helices 3 to 5 serving as the key interface following dissociation of corepressor complexes and association of coactivator complexes (Freedman, 1999; Glass and Rosenfeld, 2000; McKenna and O'Malley, 2002; Yanagisawa et al., 2002). The angle of H12 shifting in the type I NR is believed to depend on the features of ligands, generating tissue-specific actions of synthetic ligands like selective estrogen receptor modulators through ligand-specific recruitment of coregulators and complexes (Brzozowski et al., 1997).

In a previous report, we had established a *Drosophila* SBMA model by introducing the expanded polyQ hAR gene and showed that like the other expanded polyQ mutant human proteins expressing in *Drosophila* eyes, the hAR polyQ mutant AR caused an SBMA-neurodegenerative phenotype, rough eye, in an androgen-dependent manner (Takeyama et al., 2002). The molecular basis that the ligand-bound hAR polyQ mutants cause neurodegeneration in human brains as well as fly eyes still remains elusive, and androgen responsiveness might be different between fly eyes and human brains. However, considering that the onset of the neurodegeneration is caused by androgen binding to the hAR polyQ mutants, together with the observations that the structural alterations of most NR LBDs by ligand binding depend on the ligand type (Brzozowski et al., 1997), using this fly SBMA model, we can assess if the ligand-induced neurodegeneration via the hAR polyQ mutant is coupled with the transactivation function.

To test this idea, the present study was undertaken to test whether known hAR antagonists and their structure-related compounds exhibit the expected antagonistic activity in the *Drosophila* SBMA model. Surprisingly, the known antagonists failed to inhibit the ligand-induced neurodegeneration in the fly eyes. Among the tested ligands, RU56279 was found as the most potent inducer of the SBMA phenotype in our model. However, we could confirm the expected antagonistic activities of these compounds in mammalian systems. Thus, these findings suggest the presence of a novel ligand-induced function of the polyQ hAR mutant in neurodegeneration that could not be prevented by known antagonists for the hAR transactivation.

Materials and Methods

Chemicals. Dihydrotestosterone (DHT) was purchased from Fluka AG (Buchs, Switzerland). [^{3}H]Mibolerone was purchased from GE Healthcare (Little Chalfont, Buckinghamshire, UK). Testosterone propionate was purchased from Nakarai Tesque (Kyoto, Japan). Hydroxyflutamide (HF), bicalutamide (BIC), nilutamide (NIL), RU56279 (RU), and their structure-related compounds *N*-[4-cyano-3-(trifluoromethyl)phenyl]-2-hydroxy-2-methyl-3-(pyridin-2-ylthio)propanamide; *N*-[4-cyano-3-(trifluoromethyl)phenyl]-3-(ethylsulfonyl)-2-hydroxy-2-methylpropanamide; *N*-[4-cyano-3-(trifluoromethyl)phenyl]-2-hydroxy-2-methylpropanamide; 2-{[4-cyano-3-(trifluoromethyl)phenyl]amino}-1,1-dimethyl-2-oxoethyl acetate; 4-(5-imino-3,4,4-trimethyl-2-thioxoimidazolidin-1-yl)-2-(trifluoromethyl)benzonitrile; 2-(trifluoromethyl)-4-(3,4,4-trimethyl-5-oxo-2-thioxoimidazolidin-1-yl)benzonitrile; 4-[3-(4-hydroxybutyl)-5-imino-4,4-dimethyl-2-thioxoimidazolidin-1-yl]-2-(trifluoromethyl) benzonitrile; 4-(5-imino-4,4-dimethyl-2-oxoimidazolidin-1-yl)-2-(trifluoromethyl)benzonitrile; and 2-(trifluoromethyl)-4-(3,4,4-trimethyl-2,5-dioxoimidazolidin-1-yl)benzonitrile were synthesized at Yamanouchi Pharmaceutical Co., Ltd (Tokyo, Japan).

***Drosophila* Stocks and Generation of Transgenic Flies.** All general fly stocks and the *ptc-GAL4* line were obtained from the Bloomington *Drosophila* Stock Center (Indiana University, Bloomington, IN). Transgenic constructs, together with pπ 25.7 wc transposase, were microinjected into 5- to 30-min-old w^{1118} embryos reared at 18°C, using a micromanipulator (Leica, Wetzlar, Germany). Several transgenic lines were generated (Tsuneizumi et al., 1997). The AR mutant cDNAs in pCaSpeR3 and an ARE-GFP reporter construct (GFP-TT in pCaSpeR3 with a consensus ARE in its promoter) were specifically constructed for microinjection into *Drosophila*. Plasmid rescue and sequencing were performed to confirm the presence of AR mutants in the transgenic lines. Target chromosomes were separated from those carrying the GAL4 driver by crossing with flies harboring second and third balancer chromosomes *CyO* and *TM3*, respectively. The *GMR-GAL4* line, expressing GAL4 in the retina driven by the glass multimer reporter, was used as the GAL4 driver line (Moses and Rubin, 1991). The *UAS-Q127* lines were the generous gift of Dr. Parsa Kazemi-Esfarjani (Department of Physiology and Biophysics, University at Buffalo, The State University of New York, Buffalo, NY) (Kazemi-Esfarjani and Benzer, 2000).

Immunofluorescence and Histology. Tissues were dissected and fixed for 20 min in 4% formaldehyde (Tanimoto et al., 2000) and incubated with a primary antibody, hAR (N-20), that recognized the N-terminal A/B domain of AR (Santa Cruz Biotechnology, Inc., Santa Cruz, CA). Cy5-conjugated AffinityPure donkey anti-rabbit IgG (Jackson ImmunoResearch Laboratories, West Grove, PA) was used as the secondary antibody for immunofluorescence staining. Confocal microscopy was performed with a Zeiss confocal laser scanning system 510 (Zeiss, Oberkochen, Germany). For scanning electron microscopy (SEM) images, whole flies were dehydrated in ethanol, critical-point dried, and analyzed with a JSM 5400 microscope (JEOL, Tokyo, Japan).

Western Blot Analysis. To detect hAR and GFP expression in *Drosophila*, cell lysates from the heads of adult flies or third instar larvae with or without ligand were separated by 7.5% SDS-polyacrylamide gel electrophoresis and detected with hAR (N-20) antibody and GFP antibody (Santa Cruz Biotechnology, Inc.), and expression levels were measured using Adobe Photoshop software facility. -Fold activation of hAR in *Drosophila* was shown as GFP expression signal intensity normalizing with hAR expression signal intensity.

Binding Assay for Rat Androgen Receptor. The ventral prostate gland was obtained from 20-week-old male Wistar rats 24 h after castration. The homogenized tissue was spun at 800*g* for 20 min. Next, the supernatant was subjected to further centrifugation at 223,000*g* for 60 min, and the resulting supernatant was recovered to obtain the cytosol fraction. The cytosol fraction was adjusted to a protein concentration of 1 mg/ml and used as a rat androgen receptor solution. [^{3}H]Mibolerone, triamcinolone acetate (Sigma-Aldrich, St. Louis, MO), and dimethyl sulfoxide (DMSO; Nakarai Tesque) were added to 400 μl of the rat androgen receptor solution to final concentrations of 1 nM, 1 μM, and 5%, respectively, and the final volume was adjusted to 0.5 ml. After 18 h at 4°C, this solution was mixed

with 500 μl of a solution containing 0.05% of Dextran-T70 (GE Healthcare) and 0.5% of Darco G-60 (Wako Pure Chemical Industries, Osaka, Japan). This mixture was incubated at 4°C for 15 min and then subjected to centrifugation at 1500*g* for 15 min to recover the supernatant. A 600-μl portion of the recovered supernatant was mixed with 5 ml of Aquasol-2 (PerkinElmer Life and Analytical Sciences, Boston, MA), and then the radioactivity was measured to calculate the total amount of [^{3}H]mibolerone that bonded to the rat androgen receptor. The amount of nonspecific binding was calculated in the same manner by adding a DMSO solution containing unlabeled mibolerone at a final concentration of 40 μM. The difference between the total binding amount and the nonspecific binding amount was defined as the specific binding amount. The specific binding amount of [^{3}H]mibolerone bound to the rat androgen receptor in the presence of a compound was calculated by adding a DMSO solution containing various concentrations of the compound, simultaneously with [^{3}H]mibolerone, and carrying out a similar reaction as described above. The IC_{50} value of the inhibition activity of the compound on the specific binding of [^{3}H]mibolerone was obtained by nonlinear analysis using the Statistical Analysis System (SAS Institute, Cary, NC). Also, the dissociation constant K_i was calculated from the IC_{50} value by the formula of Cheng and Prusoff (1973).

Evaluation of Transcriptional Activity for the Human Androgen Receptor. CHO cells were transfected at 40 to 70% confluence in 10-cm Petri dishes with a total of 20 μg of hAR expression and reporter plasmids (pMAMneo*LUC*, MMTV-luciferase reporter plasmid, BD Biosciences Clontech, Palo Alto, CA; and pSG5-hAR, human androgen receptor expression plasmid; or SV40-LUC, SV40-luciferase reporter plasmid containing the neomycin-resistant gene) by calcium phosphate-mediated transfection (Furutani et al., 2002; Kinoyama et al., 2004). The transfected cells were selected in the culture medium supplemented with neomycin. The stable transformants that had high expression of hAR were designated as AR/CHO#3 or SV/CHO#10, respectively (Furutani et al., 2002).

The AR/CHO#3 or SV/CHO#10 cells were plated onto 96-well luminoplates at a density of 20,000 cells/well. Four to 8 h later, the medium was changed to the medium containing DMSO, 0.3 nM DHT, or 0.3 nM DHT and a compound. At the end of the incubation, the medium was removed, and then the cells were lysed with 20 μl of lysis buffer [25 mM Tris-HCl (pH 7.8), 2 mM dithiothreitol, 2 mM 1,2-cyclohexanediamine-tetraacetic acid, 10% glycerol, and 1% Triton X-100]. Luciferase substrate [20 mM Tris-HCl (pH 7.8), 1.07 mM $(MgCO_3)4Mg(OH)2.5H_2O$, 2.67 mM $MgSO_4.7H_2O$, 0.1 mM EDTA, 33.3 mM dithiothreitol, 0.27 mM coenzyme A, 0.47 mM luciferin, and 0.53 mM ATP] was added, and luciferase activity was measured with an ML3000 luminometer (Dynex Technologies, Chantilly, VA).

Yeast Two-Hybrid System and β-Galactosidase Assay. The pGBT9(GAL4-DBD)-AR(EF) fusion plasmid was constructed by inserting human AR-EF regions into the pGBT9 vector (BD Biosciences Clontech). ARA70 cDNA was inserted into pGAD10 (BD Biosciences Clontech), which included a GAL4 transactivation domain, to construct pGAD-ARA70. The pGBT9(GAL4-DBD)-AR(EF) plasmid was cotransformed with pGAD-ARA70 into *Saccharomyces cerevisiae* Y153 (MATa gal4 gal80 his3 trp1–901 ade2–101 ura3–52 leu2–3 leu2–112 URA3::GAL HIS3) by the lithium acetate method. Transformants were plated in medium lacking leucine and tryptophan and were grown overnight in 2 ml of selective dropout medium lacking leucine and tryptophan. These samples, diluted to an optical density at 600 nm of 0.02, were cultured overnight with compounds. Cells were then harvested and assayed for β-galactosidase activity as described previously (Takeyama et al., 1999).

GST Pull-Down Assay. Human AR A/B domain (AF-1) and its Q52 mutant (Q52 AF-1) were expressed as GST fusion proteins [GST-AR(AF-1) and GST-AR(Q52 AF-1), respectively] in *Escherichia coli*, as previously described, and bound to glutathione-Sepharose 4B beads (GE Healthcare, Piscataway, NJ). The ^{35}S-labeled AR deletion mutant, together with DNA and ligand binding domains CDE/F, were incubated with beads bound with either GST-AR(AF-1) or GST-AR(Q52 AF-1) in the absence or presence of 10^{-6} M RU in NET-N buffer [0.5% Nonidet P-40, 20 mM Tris-HCl(pH 7.5), 200 mM NaCl, 1 mM EDTA] with 1 mM phenylmethylsulfonyl fluoride. Bound proteins were separated by 9% SDS-polyacrylamide gel electrophoresis and lightly stained with Coomassie Brilliant Blue to verify equal protein loading and then visualized by autoradiography.

Antiandrogenic Activity in Castrated Immature Male Rats. Male Wistar Rats (Charles River Japan, Yokohama, Japan) weighing 75 to 90 g were used. The animals were given ordinary laboratory food and tap water ad libitum and housed under artificial light for 13 h/day (from 7:30 AM to 8:30 PM). All experiments were performed in compliance with the regulations of the Animal Ethical Committee of Yamanouchi Pharmaceutical. The rats were castrated and administered orally either compounds or vehicle and subcutaneously either vehicle or testosterone propionate for 5 consecutive days. The day following the last administration, the rats were weighed and necropsied. The ventral prostate of each rat was excised and weighed.

Results

None of the Known hAR Antagonists and Their Derivatives Could Block the Ligand-Induced Neurodegeneration in the Fly SBMA Model. We had previously established the *Drosophila* SBMA model by expressing a human androgen receptor (hAR) gene containing expanded polyglutamine stretches (52 residues) [*hAR(Q52)* line] in fly eyes by the *GAL4-UAS* system (Takeyama et al., 2002). In this fly line, which also carries an exogenous GFP reporter gene with a consensus androgen response element (ARE) in the promoter (Fig. 1A), hAR(Q52) is ectopically expressed in eye neurons by a glass multimer receptor (*GMR*) gene promoter. The expression of hAR(wt) and hAR(Q52) protein, the construct of which were shown in Fig. 1B, was confirmed by immunohistochemistry with a specific hAR antibody and appears red (Fig. 1C). The androgen DHT response in hAR(Q52) in the fly eyes was observed by GFP expression and appears green, like in the wild-type hAR-expressing fly eyes (see Fig. 1C). Expression of hARs and GFP proteins in eyes were further confirmed by Western blotting in total eye extracts (Fig. 1, D and E). Using this model, we evaluated several known hAR antagonists and several of their structure-related compounds. In the flies expressing wild-type hAR [hAR(wt) line], neither phenotypic abnormalities (representative data by DHT and RU are shown in Fig. 2A) nor significant GFP expression (quantitative data of representative observations of AR and GFP protein expressions by BIC, HF, NIL, and RU were shown in Fig. 2B) was induced by the tested compounds. The compounds were then ingested by the hAR(Q52) line together, with or without DHT. Similar responses to DHT and synthetic ligands monitored as GFP expressions, which monitor the transactivation function of wild-type hAR, were observed in the hAR mutant (Fig. 2D). When ingested together with DHT, however, no compounds failed to antagonize the DHT action to induce the rough eye phenotype (Fig. 2C). Furthermore, surprisingly, all of the known AR antagonists and the structure-related compounds alone were capable of inducing the rough eye phenotype in the hAR(Q52) line (Fig. 3A). Through a light microscope (LM) and scanning electron microscope (SEM), the eyes of the hAR(Q52) line that ingested these compounds had reduced ommatidia and lost pigmentation, which are typical neurodegenerative phenotypes (Figs. 2C and 3A). Although all the compounds antagonized the DHT action to induce the trans-

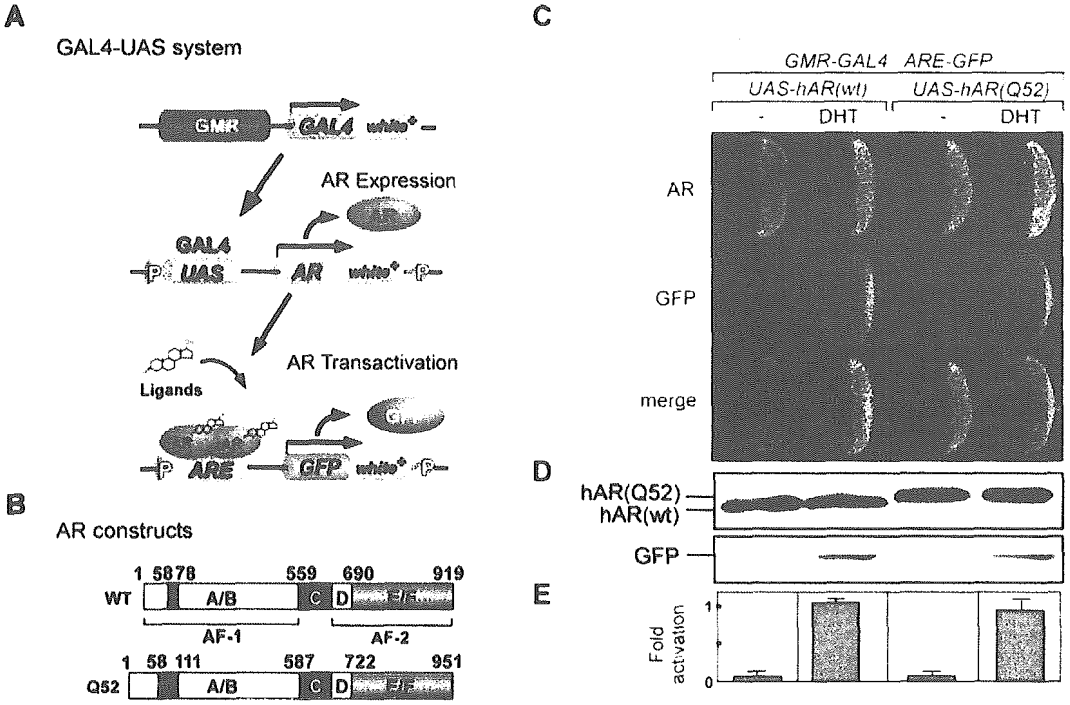

Fig. 1. Ectopic expression of functional human androgen receptors in *Drosophila* eyes. A, expression of human AR proteins in *Drosophila* eyes using the *GAL4-UAS* system. To monitor the ligand-induced transactivation of hAR proteins, hAR-expressing flies are further crossed to flies carrying a GFP reporter gene. GFP expression was induced by ligand-bound hAR that binds at the consensus ARE in the GFP receptor gene promoter. B, human AR constructs. Location of the polyglutamine region (red boxes) in relation to the DNA binding domain (black boxes, C domain) is shown. Transactivation function 1 region is localized within the N-terminal A/B domain, and transactivation function 2 region is localized within C-terminal E/F domain. C, ligand-induced transactivation of hARs in eye discs. Expression of hAR in third instar larva eye discs driven by *GMR-GAL4* was detected with hAR antibody (N-20) (red). Transactivation of hAR was estimated by GFP expression (green). D, human AR and GFP expression in four pairs of total adult heads as detected by Western blotting. E, -fold activation was calculated using hAR expression levels as normalizing factor. DHT was added at 10^{-5} M in fly diet during larval stage for ingestion.

activation of hAR mutant (Fig. 2D), it is notable that the content of hAR proteins in the eyes of the hAR(Q52) and the hAR(wt) lines appear unchanged after compound ingestion (Fig. 2, B and D). However, we could not exclude a possible difference in ligand response between fly eyes and human tissues.

Among the tested compounds, we found that 4-(4,4-dimethyl-2,5-dioxo-1-imidazolidinyl)-2-trifluoromethylbenzonitrile, previously designated as RU56279 (Cousty-Berlin et al., 1994), induced the rough eye phenotype of hAR(Q52) more potently than any other tested compound (Figs. 2C and 3A). RU56279 is a structure-related compound of nilutamide that is also used as a hAR antagonist for clinical treatment of prostate cancer. To address whether the effect of RU56279 to induce the rough eye phenotype mediates the hAR polyQ mutant, we examined the RU56279 effects on the eyes in wild-type flies and the transgenic fly expressing a 127 polyQ protein that develops rough eyes without any AR ligand treatment (127Q line) (Kazemi-Esfarjani and Benzer, 2000). The rough eye phenotype of the 127Q flies was not enhanced by RU56279 (Fig. 3B), and RU56279 exhibited no action in the parent wild-type fly line (*GMR-GAL4*). Together with the inability of RU56279 to induce neurodegeneration in the eyes of hAR(wt), the RU56279 effect appeared to mediate the polyQ hAR mutant.

RU56279 Antagonized the DHT-Induced Transactivation Function of hARs in Mammalian Systems. Although RU56279 was reported as a metabolite of RU56187 with antiandrogenic activity in the rat model (Cousty-Berlin et al., 1994), its characterization as a hAR ligand, including in vitro evaluation, remained to be investigated. A binding assay for hAR showed that RU56279 binds to AR in the nanomolar range, with a K_i value of 34.2 nM (Fig. 4A). Next, we examined whether RU56279 acts as a hAR agonist or antagonist using CHO cells stably expressing the hAR vector together with an MMTV-luciferase reporter construct. RU56279 inhibited the DHT-induced transcription in a dose-dependent manner, although RU56279 alone did not stimulate transcription (Fig. 4B). Such RU56279-antagonistic actions to transiently expressed hAR were also observed in HeLa, Cos1, and 293F cells (data not shown). Next, the RU56279 effect on the ligand-induced interaction of hAR and ARA70, which is a reported coregulator protein of hAR as a direct interactant in a yeast two-hybrid system, was examined (Yeh and Chang, 1996). RU56279 did not induce the interaction of ligand-bound hAR with ARA70 in yeast, whereas DHT binding could induce the interaction (Fig. 4C), although RU56279 disrupted the DHT-induced interaction of the hAR and ARA70 in a dose-dependent manner as well as other known antagonists. Moreover, ligand-induced alterations of the hAR structure were directly analyzed using a GST pull-down assay. As shown Fig. 4D, RU could not induce interactions between A/B (AF-1) and E/F (AF-2) domains for hAR(wt) and hAR(Q52). The results of RU56279 shown in this experiment were similar to that of HF as reported previously (Takeyama et al., 2002). Finally, to test the RU56279-antagonistic activity in androgen-dependent prostate development, RU56279 was administered to castrated rats that were supplemented with testosterone propionate. RU56279

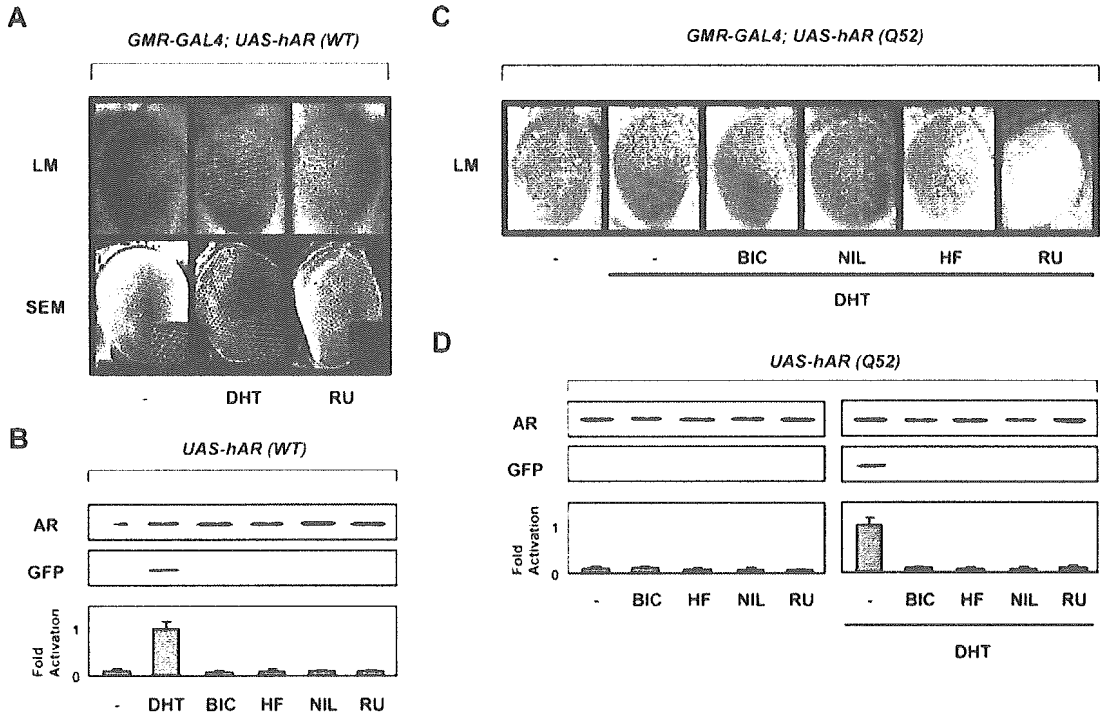

Fig. 2. Agonist-induced rough eyes in the fly line expressing human polyQ AR mutant. A, effect of ligands on the eyes of hAR(wt) fly line. The panels show the LM and SEM images of adult eyes of 5-day-old flies treated with the indicated ligands. B, effect of ligands on transactivation of wild-type hAR in eye imaginal discs. The panels show the hAR and GFP expressions in four pairs of adult eyes at 5 days old. Ligands [10^{-5} M DHT, BIC, HF, NIL, or RU] were treated during larval stage. -Fold activation by ligands was calculated using hAR expression levels as a normalizing factor. C, known antagonists were unable to attenuate the androgen-induced rough eye phenotype in the hAR(Q52) fly line. LM images of adult eyes of 5-day-old flies treated as the indicated ligands are shown. D, effect of ligands on transactivation of mutant hAR in eye imaginal discs. The panels show the mutant hAR and GFP expression in four pairs of adult eyes of 5-day-old flies. -Fold activation was calculated using hAR expression levels as a normalizing factor.

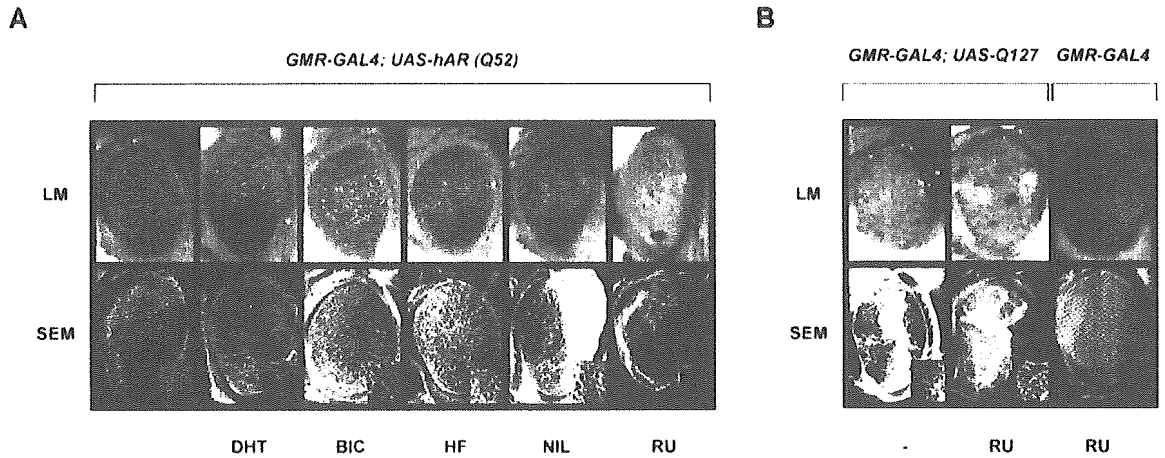

Fig. 3. Antagonist-induced rough eyes in the fly line expressing human polyQ AR mutant. A, known antagonists alone were potent to induce neurodegeneration of the hAR(Q52) fly eyes. LM and SEM images of adult eyes of 5-day-old flies treated with ligands during larval stage are shown. B, no additive action of RU56279 in the rough eye phenotype of the Q127 fly line. LM and SEM images of adult eyes from 5-day-old flies treated as larva with RU are shown. Genotype is *UAS-127Q* in trans to *GMR-GAL4* and *GMR-GAL4*.

antagonized the testosterone action in prostate growth (Fig. 4E). Together with the known antagonists exhibiting the expected actions to antagonize the androgen actions in mammalian systems (data not shown), these findings suggest that RU56279 is an androgen antagonist in mammalian systems.

Discussion

***Drosophila* as a Transgenic Animal Model to Study Human Steroid Hormone Receptors.** AR belongs to the NR gene superfamily and acts as a ligand-inducible transcription factor. Since AR is believed to play a central role in androgen signaling pathways, any malfunction of AR tends to cause certain disorders. The physiological and pathological impacts of AR could be tested in a mouse model by disrupting the AR gene in a given tissue and overexpressing the gene transgenically (Chatterjee et al., 1996; Kawano et al., 2003; Sato et al., 2003, 2004). However, the AR mutants, like the ones with expanded polyQ residues, are not easily studied

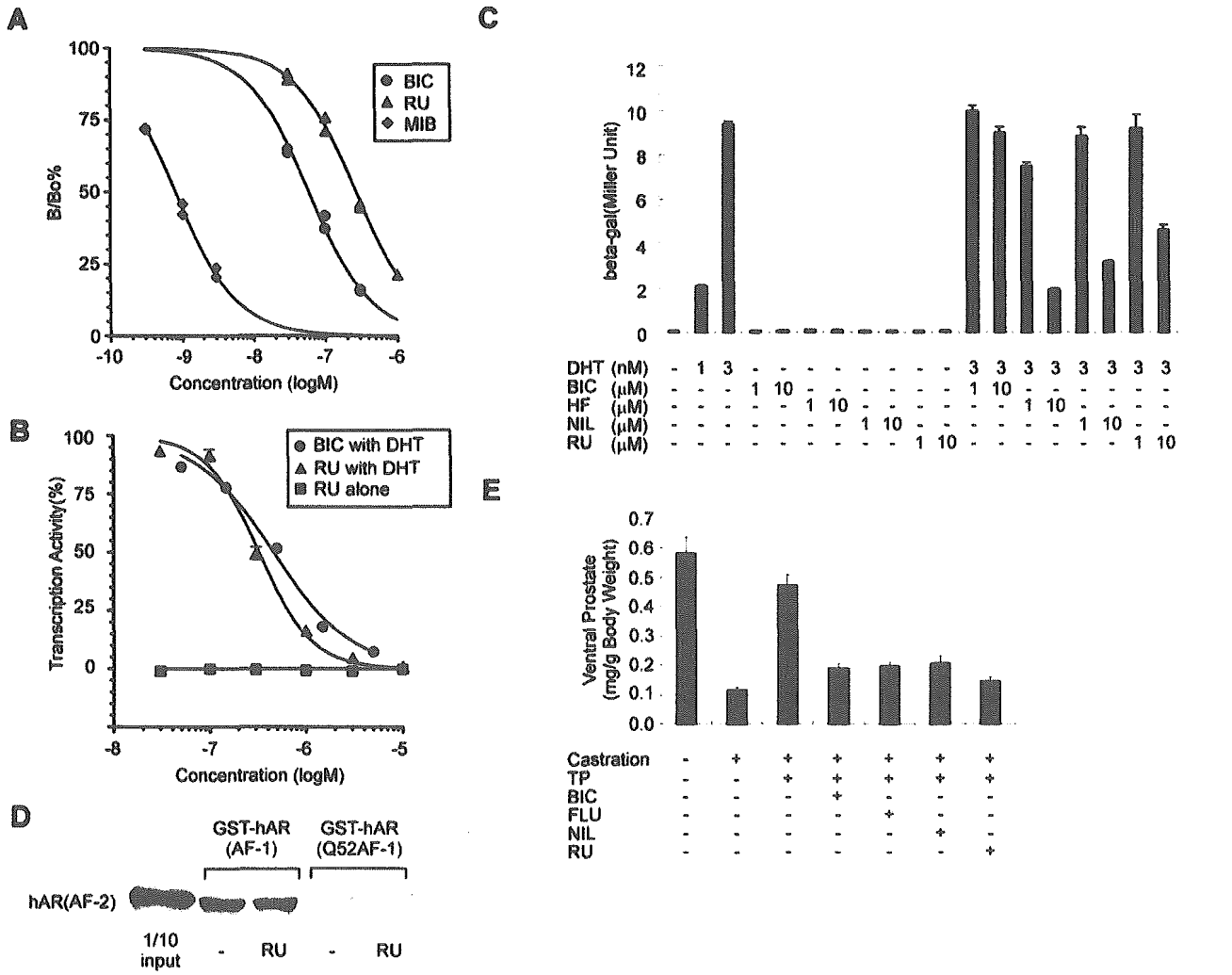

Fig. 4. Antiandrogenic actions of the known antagonist RU56279 in in vitro and in vivo mammalian systems. A, competitive binding of androgen antagonists with an agonist in the rat prostate cytosols. The rat prostate cytosols were incubated with unlabeled MIB, BIC, or RU at the indicated concentrations with 1 nM [^{3}H]mibolerone (a hAR agonist). The radioactivity was measured as described under *Materials and Methods*. Data are expressed as duplicate determinations. B, RU56279 as a hAR antagonist for hAR transactivation function. The stable transformant of CHO cells, which contain the human AR gene and MMTV-luciferase reporter gene (Furutani et al., 2002), were treated with either BIC or RU at the indicated concentrations in the presence or absence of DHT at 0.3 nM. After 18 h, cells were harvested and assayed for luciferase activity as described under *Materials and Methods*. Data are expressed as the mean ± S.E.M. of triplicate determinations. C, RU56279 inhibited the androgen-induced interaction of human AR with a hAR cofactor in the yeast two-hybrid system. pGBT9(GAL4-DBD)-AR(EF) fusion protein and pGAD10(GAL4-AD)-ARA70 fusion protein (Yeh and Chang, 1996) were expressed in yeast containing the lacZ gene controlled by the GAL4 enhancer. The yeast cells were treated with either BIC, HF, NIL, or RU at the indicated concentrations in the presence or absence of DHT. Interaction of hAR with the cofactor was assessed by measuring β-galactosidase activity. Data are expressed as the mean ± S.E.M. of triplicate determinations. D, effects of RU56279 on interaction of hAR(AF-2) and hAR(Q52 AF-1) in vitro. Interaction was assessed by incubating a GST fusion protein with either hAR(AF-1) [GST-hAR(AF-1)] and mutant hAR(AF-1) with Q52 [GST-hAR(Q52 AF-1)] with in vitro-translated [^{35}S]methionine-labeled hAR LBD [hAR(AF-2)] by pcDNA3-hAR 560-919. E, RU56279 on rat prostate growth as an androgen-antagonist. Male Wistar rats were castrated and then treated with testosterone propionate (TP) along with the indicated antagonists daily for 5 days. The rats were sacrificed, and ventral prostates were removed and weighed. Data are expressed as the mean ± S.E.M. obtained from five rats. FLU, flutamide.

through mouse genetics due to the time required for the identification of the coregulator responsible for hAR function and screening of a novel ligand to restore the impaired AR functions. We have established a number of fly lines expressing hARs and other mammalian steroid hormone receptors and found that ectopic expression of these NRs is quite safe for fly life, even in the presence of the cognate hormone (Takeyama et al., 2002; Ito et al., 2004; Kouzmenko et al., 2004). The major reason for this safety may be explained by mammalian exogenous steroid hormone receptors binding to exogenous DNA as a homodimer and, therefore, not competing for endogenous DNA binding sites for endogenous fly NR heterodimers, since the DNA elements recognized between NR homodimers and heterodimers are distinct (Mangelsdorf et al., 1995; McKenna and O'Malley, 2002).

No Known hAR Antagonist Could Block the Ligand-Induced Neurodegeneration in Fly Eyes by the hAR polyQ Mutant. In our previous report, we showed in fly eyes that the onset of neurodegeneration caused by the hAR polyQ mutants is dependent on DHT binding with structural alterations (Takeyama et al., 2002). Since the ligand-independent function of the polyQ-included A/B domain in the ΔLBD polyQ hAR mutants is potent enough to induce the rough eye phenotype, we presume that the ligand-induced exposure of

the polyQ repeats in the hAR A/B domain, which is apparently masked by unliganded hAR LBD, is a critical trigger step that initiates neurodegeneration. Therefore, for preventing the onset of neurodegeneration in SBMA patients, developing a novel hAR ligand not to induce the A/B domain exposure after the ligand-induced structural alteration is mandatory. Although we could not exclude a possible difference in the AR ligand response between human neurons and fly eyes, the neurodegenerative fly eyes have been applied as human models for hereditary disease caused by unusual expansions of polyQ, and the fly eye phenotype by hAR polyQ mutants was undiscriminative at histological and biochemical levels from those by the other polyQ mutants.

In the present study, we evaluated AR antagonists and structure-related compounds using the hAR(Q52) *Drosophila* line as an SBMA model. Surprisingly, no compounds were able to antagonize the DHT-induced rough eye phenotype, and among them, RU56279 was found as the most potent to induce neurodegeneration. Clearly, these compounds appear potent to induce structural alterations of the A/B domain, although they expectedly acted as antagonists on the hAR transactivation function in the mammalian systems as well as in the fly eyes. It is also likely that RU56279 is a novel AR ligand that alters the structure of the hAR mutant in a manner different from the other AR ligands, although the molecular basis of the difference in the ligand-induced structural alterations among the hAR ligands remains unclear.

A Novel Mechanism of Ligand-Induced Neurodegeneration by the hAR polyQ Mutant. The molecular mechanism of neurodegeneration by expanded polyQ proteins remains elusive, and recently, the cellular aggregates of the polyQ mutant fragments have been shown as a protective response for cell death (Arrasate et al., 2004). Unlike the other polyQ mutants, the hAR mutant neurodegenerative function is ligand-inducible, although the neuronal abnormality through the expanded polyQ residues looks indistinguishable among the polyQ mutants. Ligand-induced alteration of the hAR mutants is presumed to trigger such pathological processes in neurons; however, any coregulators responsible for the pathological function of the hAR mutants are unknown. Since ligand-induced transactivation of the wild-type hAR as well as the hAR polyQ mutants is believed to require a number of transcriptional coregulators and complexes, it is possible to speculate that the ligand-bound hAR polyQ mutants either recruit a critical initiator for neurodegeneration or dissociate from a protective factor. Moreover, it may be possible to identify such factors using and investigating the hAR antagonists, especially RU56279. In any case, identification of such a factor is required for revealing the molecular mechanism of the androgen-induced neurodegeneration via hAR polyQ mutants, and this fly SBMA model should be powerful for the genetic screening of the coregulators (Takeyama et al., 2004). Most notably, a novel class of ligand may be developed based on inhibition of physical and/or functional interaction of the hAR polyQ mutants with the identified factor, and such an idea should be addressed in human SBMA patients. The present study clearly suggests that the hAR(Q52) fly lines are a novel tool to screen a new class of hAR synthetic ligands, particularly the antagonist for the hAR polyQ mutants in neurodegeneration suffered in SBMA patients.

Acknowledgments

We are grateful to all members of the Pharmacology Laboratories, Chemistry Laboratories, and the Molecular Medicine Laboratories in Yamanouchi Pharmaceutical Co., Ltd. for encouragement and support. We also thank H. Higuchi for manuscript preparation.

References

Arrasate M, Mitra S, Schweitzer ES, Segal MR, and Finkbeiner S (2004) Inclusion body formation reduces levels of mutant huntingtin and the risk of neuronal death. *Nature (Lond)* **431:**805–810.

Brzozowski AM, Pike AC, Dauter Z, Hubbard RE, Bonn T, Engstrom O, Ohman L, Greene GL, Gustafsson JA, and Carlquist M (1997) Molecular basis of agonism and antagonism in the oestrogen receptor. *Nature (Lond)* **389:**753–758.

Chatterjee B, Song CS, Jung MH, Chen S, Walter CA, Herbert DC, Weaker FJ, Mancini MA, and Roy AK (1996) Targeted overexpression of androgen receptor with a liver-specific promoter in transgenic mice. *Proc Natl Acad Sci USA* **93:**728–733.

Cheng Y and Prusoff WH (1973) Relationship between the inhibition constant (K1) and the concentration of inhibitor which causes 50 per cent inhibition (I50) of an enzymatic reaction. *Biochem Pharmacol* **22:**3099–3108.

Choong CS and Wilson EM (1998) Trinucleotide repeats in the human androgen receptor: a molecular basis for disease. *J Mol Endocrinol* **21:**235–257.

Cousty-Berlin D, Bergaud B, Bruyant MC, Battmann T, Branche C, and Philibert D (1994) Preliminary pharmacokinetics and metabolism of novel non-steroidal antiandrogens in the rat: relation of their systemic activity to the formation of a common metabolite. *J Steroid Biochem Mol Biol* **51:**47–55.

Freedman LP (1999) Increasing the complexity of coactivation in nuclear receptor signaling. *Cell* **97:**5–8.

Furutani T, Watanabe T, Tanimoto K, Hashimoto T, Koutoku H, Kudoh M, Shimizu Y, Kato S, and Shikama H (2002) Stabilization of androgen receptor protein is induced by agonist, not by antagonists. *Biochem Biophys Res Commun* **294:**779–784.

Glass CK and Rosenfeld MG (2000) The coregulator exchange in transcriptional functions of nuclear receptors. *Genes Dev* **14:**121–141.

He B, Kemppainen JA, Voegel JJ, Gronemeyer H, and Wilson EM (1999) Activation function 2 in the human androgen receptor ligand binding domain mediates interdomain communication with the NH(2)-terminal domain. *J Biol Chem* **274:**37219–37225.

Ito S, Takeyama K, Yamamoto A, Sawatsubashi S, Shirode Y, Kouzmenko A, Tabata T, and Kato S (2004) In vivo potentiation of human oestrogen receptor alpha by Cdk7-mediated phosphorylation. *Genes Cells* **9:**983–992.

Kato S, Endoh H, Masuhiro Y, Kitamoto T, Uchiyama S, Sasaki H, Masushige S, Gotoh Y, Nishida E, Kawashima H, et al. (1995) Activation of the estrogen receptor through phosphorylation by mitogen-activated protein kinase. *Science (Wash DC)* **270:**1491–1494.

Kawano H, Sato T, Yamada T, Matsumoto T, Sekine K, Watanabe T, Nakamura T, Fukuda T, Yoshimura K, Yoshizawa T, et al. (2003) Suppressive function of androgen receptor in bone resorption. *Proc Natl Acad Sci USA* **100:**9416–9421.

Kazemi-Esfarjani P and Benzer S (2000) Genetic suppression of polyglutamine toxicity in Drosophila. *Science (Wash DC)* **287:**1837–1840.

Kinoyama I, Taniguchi N, Yoden T, Koutoku H, Furutani T, Kudoh M, and Okada M (2004) Synthesis and pharmacological evaluation of novel arylpiperazine derivatives as nonsteroidal androgen receptor antagonists. *Chem Pharm Bull (Tokyo)* **52:**1330–1333.

Kouzmenko AP, Takeyama K, Ito S, Furutani T, Sawatsubashi S, Maki A, Suzuki E, Kawasaki Y, Akiyama T, Tabata T, and Kato S (2004) Wnt/beta-catenin and estrogen signaling converge in vivo. *J Biol Chem* **279:**40255–40258.

La Spada AR, Wilson EM, Lubahn DB, Harding AE, and Fischbeck KH (1991) Androgen receptor gene mutations in X-linked spinal and bulbar muscular atrophy. *Nature (Lond)* **352:**77–79.

Mangelsdorf DJ, Thummel C, Beato M, Herrlich P, Schutz G, Umesono K, Blumberg B, Kastner P, Mark M, Chambon P, and Evans RM (1995) The nuclear receptor superfamily: the second decade. *Cell* **83:**835–839.

McKenna NJ and O'Malley BW (2002) Combinatorial control of gene expression by nuclear receptors and coregulators. *Cell* **108:**465–474.

Merry DE and Fischbeck KH (1998) Genetics and molecular biology of the androgen receptor CAG repeat, in *Genetic Instability and Hereditary Neurological Disease* (Wells RD and Warren ST eds) pp 101–111, Academic Press, New York.

Mooradian AD, Morley JE, and Korenman SG (1987) Biological actions of androgens. *Endocr Rev* **8:**1–28.

Moses K and Rubin GM (1991) Glass encodes a site-specific DNA-binding protein that is regulated in response to positional signals in the developing Drosophila eye. *Genes Dev* **5:**583–593.

Poujol N, Wurtz JM, Tahiri B, Lumbroso S, Nicolas JC, Moras D, and Sultan C (2000) Specific recognition of androgens by their nuclear receptor. A structure-function study. *J Biol Chem* **275:**24022–24031.

Sato T, Matsumoto T, Kawano H, Watanabe T, Uematsu Y, Sekine K, Fukuda T, Aihara K, Krust A, Yamada T, et al. (2004) Brain masculinization requires androgen receptor function. *Proc Natl Acad Sci USA* **101:**1673–1678.

Sato T, Matsumoto T, Yamada T, Watanabe T, Kawano H, and Kato S (2003) Late onset of obesity in male androgen receptor-deficient (AR KO) mice. *Biochem Biophys Res Commun* **300:**167–171.

Shang Y, Myers M, and Brown M (2002) Formation of the androgen receptor transcription complex. *Mol Cell* **9:**601–610.

Shiau AK, Barstad D, Loria PM, Cheng L, Kushner PJ, Agard DA, and Greene GL (1998) The structural basis of estrogen receptor/coactivator recognition and the antagonism of this interaction by tamoxifen. *Cell* **95:**927–937.

Takeyama K, Ito S, Sawatsubashi S, Shirode Y, Yamamoto A, Suzuki E, Maki A,